DC-Distributed Power System Modeling and Hardware-in-the-Loop (HIL) Evaluation of Fuel Cell-Powered Marine Vessel

Wenjie Chen, *Student Member, IEEE*, Kang Tai, Michael Lau, Ahmed Abdelhakim, *Senior Member, IEEE*, Ricky R. Chan, Alf Kåre Ådnanes, and Tegoeh Tjahjowidodo

***Abstract*—Environmentally driven regulations are significantly affecting shipping in recent years, where the shipbuilding industry is required to comply with upcoming restrictions concerning polluting emissions. The all-electric ship (AES) is one of the most promising technologies for complying with the increasingly strict environmental regulations, improving fuel efficiency, and enhancing system dynamic performance. In this study, the dc-distributed power grid of an AES integrated with fuel cells and batteries has been configured using extensive electrification technology, where the system-level shipboard power plant has been modeled with the average modeling method. The model not only incorporates the hybrid power source integration but also the primary and secondary power management as a whole. In addition, a hardware-in-the-loop (HIL) has been set up to replicate the real-time system behavior, which is essential for the verification of any optimal power management control algorithms to be developed in future work. Finally, both the mathematical and real-time models are validated against the full-scale hybrid shipboard power system.**

***Index Terms*—All-electric ship, fuel cell system (AES), hardware-in-the-loop (HIL), hybrid shipboard power microgrid, renewable energy sources.**

I. Introduction

MARITIME transport has played a dominant role in the global trade system for centuries, and it is expected that international maritime trade will expand at continuous annual growth for years to come [1]. Recently, environmental sustainability has become a significant policy concern in global maritime transport [2]. With this concern, the shipbuilding industries are compelled to abide by rules on polluting emissions imposed by International Maritime Organization (IMO) and national legislation [3]. To achieve high energy efficiency and low emission, it is believed that the all-electric ship (AES) will be one of the most promising technologies to comply with the environmental regulations [4]. In particular, vessel types such as tug boats, river pushers, and ferries will be the early adopters as they usually operate near coasts or in inner rivers, which belong to emission control areas (ECAs). Other vessel types such as container vessels may need more time before the AES design can be adopted [5].

With the development of energy storage technologies, new energy sources can be integrated into the shipboard power network. Batteries, as the most mature energy storage system (ESS) device, have been widely utilized in different applications in marine vessels. However, due to energy density limitation, battery systems only function as a main power supply for small-scale vessels in short distance shipping segment or as an auxiliary power source onboard of large vessels to enhance the dynamic performance or short-term zero-emission operation. In order for clean energy sources to be a feasible solution for larger ocean-going ship types, such as cruise ships and RoRo/RoPax (the vessels built for freight vehicle transport with passenger accommodation), fuel cell systems have been introduced. It is expected that fuel cell systems would replace diesel engines as the main power source in the future.

The hybrid shipboard power system integrated with different types of power sources brings in a lot of benefits, but it also increases the complexity of the system structure and power management control. To get deep understanding of the hybrid power system and improve the current control algorithms, a comprehensive system-level hybrid power plant model is needed as a foundation. The expected system model should be able to perform the actual shipboard power plant responses under different operating modes and loading profiles.

A few power system configurations and modeling methodologies have been published in the recent literature. In [6] and [7], land-based hybrid dc microgrid configurations have

Manuscript received August 9, 2021; revised October 25, 2021, December 13, 2021, and December 17, 2021; accepted December 19, 2021. This work was supported in part by the Singapore Economic Development Board and ABB Pte. Ltd. Joint Industrial Postgraduate Program. *(Corresponding author: Wenjie Chen.)*

Wenjie Chen is with the School of Mechanical and Aerospace Engineering, Nanyang Technological University, Singapore 639798, and also with the ABB Pte. Ltd., Singapore 139935 (e-mail: wenjie003@e.ntu.edu.sg).

Kang Tai is with the School of Mechanical, and Aerospace Engineering, Nanyang Technological University, Singapore 639798 (e-mail: mktai@ntu.edu.sg).

Michael Lau is with the Newcastle University in Singapore, Singapore 599493 (e-mail: michael.lau@newcastle.ac.uk).

Ahmed Abdelhakim is with the ABB Corporate Research, 722 26 Västerås, Sweden (e-mail: ahmed.abdelhakim@se.abb.com).

Ricky R. Chan is with the Marine and Ports, ABB Oy, 1 00980 Helsinki, Finland (e-mail: ricky.chan@fi.abb.com).

Alf Kåre Ådnanes is with the Marine and Ports, ABB Engineering (Shanghai) Ltd., Shanghai 1 00980, China (e-mail: alfkare.adnanes@cn.abb.com).

Tegoeh Tjahjowidodo is with the Department of Mechanical Engineering, KU Leuven, De Nayer Campus, 2860 Sint-Katelijne-Waver, Belgium (e-mail: tegoeh.tjahjowidodo@kuleuven.be).

Color versions of one or more figures in this article are available at https://doi.org/10.1109/JESTIE.2021.3139471.

Digital Object Identifier 10.1109/JESTIE.2021.3139471

been introduced. The authors in [8] have proposed a diesel-generator-based marine power network equipped with a battery ESS, while a fuel cell-based marine system model has been developed in [9], where the authors are mainly focusing on the fuel cell chemical reaction and fuel processing. The above references focus only on certain parts of the power grid rather than the observation of the dynamics and performance of the complete system.

It is worth noting that shipboard power systems have their own special configurations and requirements [10]. The main difference with land-based power system is that shipboard power system is an isolated microgrid with short distances from generated power to the electric propulsion load [11]. The average short-circuit levels and forces are quite high so that it must be dealt with some special manners to protect the power equipment. During cruising, shipboard power system is impacted a lot by the environment, such as marine weather and unexpected thrusters load variations, therefore the system stability and reliability is crucial for marine vessels. Extra efforts in system reconfigurability and redundancy are required to prevent single point failure according to the marine classification rules. Compared to EV power system, the power scale of the shipboard power network is much bigger and complicated. Due to its particularity of the shipboard power system [12], there is the urge to build its own power plant model rather than reusing other existing models.

In addition, system-level power plant model is not only to integrate different power sources but also to implement primary and secondary level power management to coordinate power load sharing, frequency, and voltage control. A previous work by the authors [13] modeled an ac-distributed shipboard hybrid power system. However, in the past decade, dc-based distribution systems have gained popularity due to their advantages in many aspects [14]. A system-level dc-based shipboard power model is necessary to simulate the vessel operating performances. The comprehensive and reliable power plant model is the foundation and precondition for system studies and further research.

Compared to the existing studies on hybrid power network modeling problems, the main contributions of this article are highlighted as follows.

1) A dc-distributed system-level shipboard power system model is built, integrating the mathematical model of different power sources, as well as the primary and secondary power management control. All the power sources are resizable to configure the new shipboard systems according to the varied ship design specifications.
2) A hardware-in-the-loop (HIL) platform is set up in lab environment as well. HIL helps to perform the system real-time states. It is a useful tool for prototyping the power and energy management system (PEMS) controller and communication interface validation without involving any hardware devices setup.
3) Both the mathematical and real-time HIL model have been validated against the real hardware full-scale hybrid shipboard power system.

The rest of this article is organized as follows: The hybrid shipboard power system configuration is discussed in Section II. A dc-based power distribution model and the simulation results are presented in Section III. Section IV evaluates the system plant model HIL setup. And the validation tests are performed in Section V. Finally, Section VI concludes this article.

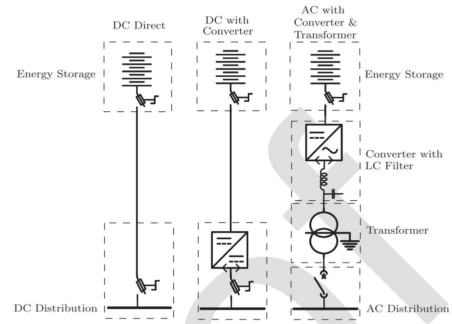

Fig. 1. ESS integration scheme for both dc and ac distribution system.

II. Shipboard Power System Configuration

In this section, the functions of several integration schemes will be introduced in detail. The advantages and the system configuration of dc-distributed shipboard power system will also be discussed.

A. Advantages of DC-Based Shipboard Power System

Currently, the majority of commercial marine vessels have a diesel or gas engine powered plant with ac distribution, while the dc-distributed shipboard system has drawn much attention over the past decade. In both ac and dc-distributed systems, ESS integration is a trend for different functionalities [15].

Energy storage, such as batteries will help the slow power devices level out load variations from the thrusters and other heavy consumers. Besides, the clean energy sources are able to provide the main power supply of the ship operation in order to achieve zero-emission operation. There are several methods to integrate the ESS into the shipboard network [16], which is shown in Fig. 1.

According to this integration scheme, it can be seen that the ESS is much easier to connect to a dc-distributed network than an ac system. The storage devices can be directly connected to the dc network. This direct-on-line (DOL) ESS gives an efficiency increase compared to the ESS with dc/dc converter, but at the cost of less control features to be achieved. On the other hand, ESS is also possible to be extended to an ac-distributed system through a dc/ac converter with LCL filter and transformer [17]. The *LCL* filter is used herein to improve the power quality and reduce the total harmonic distortion (THD) level of the main power network. While the shielded transformer is utilized to solve the electromagnetic interference (EMI) issue, it also blocks the circulating current within the power electronic converters such as IGBT or MOSFET. In addition, the dc/ac converters also need to monitor the amplitude, frequency, and phase shift of the power network voltage on ac side to achieve the synchronization operation [13]. It is clear that the ac-based power configuration is quite complex not only in system configuration but also in power management control [14]. Furthermore, it also increases

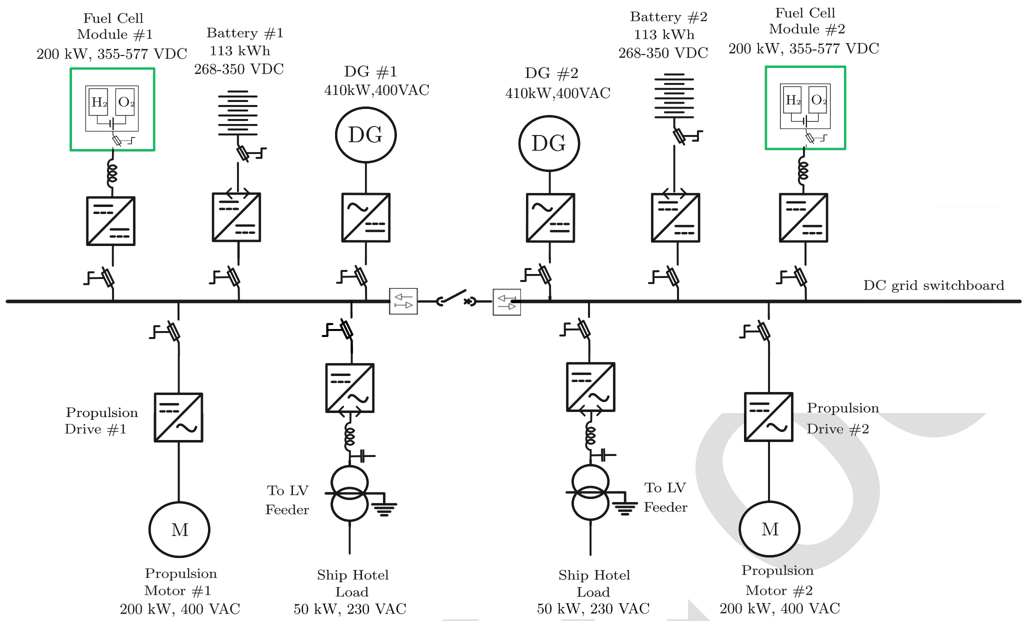

Fig. 2. Typical dc-based shipboard power system single line diagram.

the dimensions of the equipment, where the space onboard a ship is limited.

Safety is another important consideration for implementing the dc-based distribution. A dc-configured system is inherently simpler than an ac system, which means that it is easier to predict fault scenarios and devise adequate protection against them. The generators can be connected to the dc distribution system in a short time because it is not necessary for synchronization. It has considerable potential to improve the stability, efficiency, and performance of future dc-based ship power systems [18].

In addition to the benefits described above, there are numerous other benefits with dc distribution. Some of these are summarized as follows.

1) *Voltage Distortion:* Harmonic distortion is inherent in ac systems with frequency converters, while being less of a concern with dc distribution.
2) *Electrical Efficiency:* In the process of going from ac-to-dc distribution, the system efficiency is improved by 0.5–1% [19].
3) *Ease of Control:* It is not required to control the frequency and reactive power of the network. The control system is simplified and only needs to overlook the dc voltage.

Overall, the integration of a hybrid ac-distributed shipboard power is complex and costly [14]. Multiple layers of the power conversion and transmission increase the system losses and probability of equipment failure. It is more suitable for some retrofit projects, which are planned for extending a single ESS from an existing ac distribution network. Due to the advantages of dc-distribution power system, this study focuses on dc-based shipboard power plant modeling.

B. Hybrid Shipboard Power System Configuration

For a hybrid dc-distributed shipboard power system, the energy storage devices can be connected to the system. A generator set driven by a combustion diesel engine is possible to be integrated into the dc power network. Usually, synchronous generators are used and rectified (ac to dc converter) before the power is transmitted to the dc bus. Propulsion and other ship service loads are regulated by dc/ac inverters. The typical configuration of an all-electric dc hybrid ship power and propulsion system is shown in Fig. 2. In this study, two fuel cell modules are function as the main power supply to achieve zero emission operation. Two battery banks handle the ship load variations. And two diesel gen sets (DG) are the backup power in case the fuel cell devices or the hydrogen fuel are not available under emergency condition.

The main switchboards are usually split into two sections or more to obtain the redundancy requirements of the vessel according to the marine class rules and regulations. This kind of structure is not only an intrinsic advantage of dc distribution but it also has the ability to supply power to the load continuously even under certain fault conditions [16], such as short-circuit. During normal operation, the dc-grid switchboard are usually connected (close bus tie), which gives the best flexibility in the configuration of the power generation. The optimal number of the power devices can be connected to the power network according to the load transients to achieve certain control criteria.

III. Fuel Cell-Fed DC Distribution System Modeling

In this section, a system-level dc-based hybrid shipboard power plant will be modeled. The power network includes the fuel cells, batteries, and DGs as the energy sources. The essential components of the dc-grid power system are the power

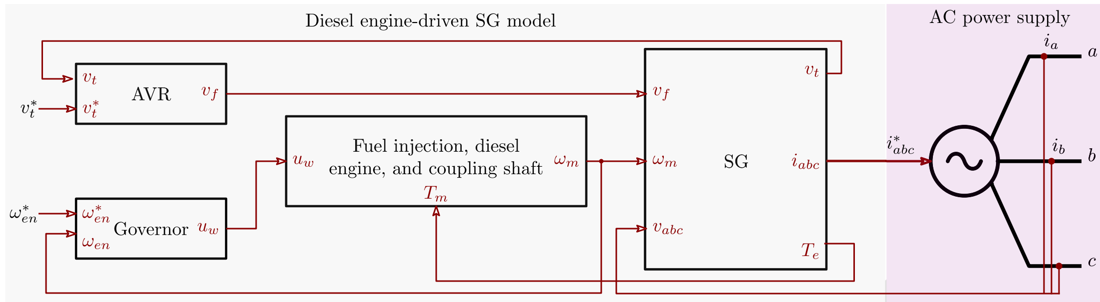

Fig. 3. General block diagram of a diesel engine-driven synchronous generator.

electronics devices. An ESS dc/dc converter and a 6-pulse ac/dc rectifier for DG integration will be modeled. The propulsion load and ship hotel loads of the vessel will be represented with controllable current sources. Power management, including load power sharing, dc voltage coordination, and power regulation will be achieved as well.

A. Energy Sources Modeling

1) *Diesel Gen-Set Model:* Fig. 3 shows the general configuration of a diesel engine-driven synchronous generator system. The system consists of four main sections: Fuel injection and diesel engine, governor, synchronous generator (SG), and automatic voltage regulator (AVR) [20]. The mathematical models of each part of diesel generator are introduced as follows.

a) *Fuel injection and diesel engine* can be presented by a time delay and the coupling shaft model, as in [21] and [22]. The simplified model is given by

$$\frac{T_m(s)}{u_\omega(s)} = \frac{K_{en} \cdot e^{-t_d \cdot s}}{t_e s + 1} \tag{1}$$

$$J_{eq} \cdot \frac{d\omega_m}{dt} = T_m - T_e - k_{f_{eq}} \cdot \omega_m \tag{2}$$

where ω_m is the mechanical speed, u_ω is the control signal from the speed governor, T_m is the mechanical torque developed by the engine, J_{eq} is the equivalent inertia of the entire system, $k_{f_{eq}}$ is the equivalent friction coefficient, K_{en} is the engine gain, t_d is a delay representing the time elapsed from the fuel injection until the torque is developed at the engine shaft, and t_e is the time constant of the fuel injection.

b) *Governor* is responsible for regulating the engine speed to maintain it within the allowable range during the different load conditions, resulting in constant output frequency or within the desired limits. This governor also has the structure of a PI controller with the droop function implemented. This model can be given by

$$u_\omega = (\omega_{en}^* - \omega_{en} - k_{dr,\text{freq}} \cdot u_\omega)\left(K_{P_\omega} + \frac{K_{I_\omega}}{s}\right) \tag{3}$$

where K_{P_ω} and K_{I_ω} are the proportional and integral gains of the governor PI controller, and ω_{en} is the engine nominal speed and $k_{dr,\text{freq}}$ is the speed droop gain that equals $(m_{dr} \cdot \omega_{en})$, and m_{dr} is the static droop slope.

c) *Synchronous generator* is considered without damper windings for the sake of simplifying the model. And its *d*-*q* rotating reference frame is given by

$$V_d = -r_s \cdot i_d + L_q \cdot \omega_e \cdot i_q + L_d \cdot \frac{di_d}{dt} + M_{sf} \cdot \frac{di_f}{dt} \tag{4}$$

$$V_q = -r_s \cdot i_q - L_d \cdot \omega_e \cdot i_d + L_q \cdot \frac{di_q}{dt} + M_{sf} \cdot \omega_e \cdot i_f \tag{5}$$

$$V_f = r_f \cdot i_f + L_f \cdot \frac{di_f}{dt} - M_{sf} \cdot \frac{di_d}{dt} \tag{6}$$

$$T_e = (L_d - L_q) \cdot i_d \cdot i_q + M_{sf} \cdot i_q \cdot i_f \tag{7}$$

where V_d, V_q, i_d, and i_q are the output voltages and currents in the *d*-*q* rotating reference frame, respectively, V_f and i_f are the field excitation voltage and current, respectively, r_s and r_f are the stator winding and field winding internal resistances, respectively, L_d and L_q are the stator inductance in the *d*-axis and *q*-axis, respectively, L_f is the inductance of the field, M_{sf} is the mutual inductance between the field winding and the *d*-axis stator winding, and T_e is the electromagnetic torque. It is worth noting that, the following assumptions have been considered: The stator windings are symmetrical, a uniform sinusoidal distribution along the air gap, the permanence of the magnetic paths on the rotor is independent of the rotor positions, and the saturation and the hysteresis effects are neglected.

d) *Automatic voltage regulator* has the responsibility of controlling the terminal voltage of the synchronous generator under different load conditions. This AVR is modeled as a first-order system, representing a power converter controlled by a PI controller [20], that is given by

$$V_f = \frac{k_{\text{conv}}}{t_{\text{conv}} s + 1} \cdot (U_v - k_{dr,v} V_f) \tag{8}$$

$$U_v = \left(K_{Pv} + \frac{K_{Iv}}{s}\right) \cdot (V_t^* - V_t) \tag{9}$$

where K_{Pv} and K_{Iv} are the proportional and integral gains of the AVR PI controller, k_{conv} and t_{conv} are the

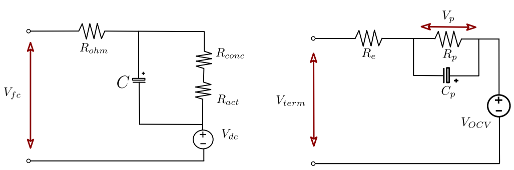

Fig. 4. ESS power source modeling. (a) Proton-exchange membrane (PEM) fuel cell and its equivalent circuit. (b) Lithium-ion battery and its equivalent circuit.

converter gain and time constant, and V_t^* and V_t are the reference and measured rms output line voltage. $k_{dr,v}$ is the dc voltage droop rate for dc-distributed power system.

2) *Fuel Cell Model:* There are a few different types of fuel cell technologies. The proton-exchange membrane (PEM) fuel cell is the most mature technology over other types of fuel cell. With its relatively low cost and high energy efficiency features, PEMFC is the most widely used in marine applications [23]. Fig. 4(a) shows a single PEM fuel cell model and its equivalent circuit [24]. The fuel cell losses are mainly divided into three categories: Activation loss R_{act}, concentration loss R_{conc}, and ohmic loss R_{ohm} [25]. The voltage of a PEMFC elementary cell can be written as follows [26]:

$$V_{\text{cell}} = E_{\text{nernst}} - V_{\text{act}} - V_{\text{conc}} - V_{\text{ohm}} \tag{10}$$

$$V_{fc} = N_{fc} \times V_{\text{cell}} \tag{11}$$

where V_{cell} is the voltage of a PEMFC elementary cell, E_{nernst} is the equilibrium voltage, V_{act} is the activation overpotential, V_{conc} is the concentration overpotential, V_{ohm} is the ohmic overpotential, V_{fc} is the voltage of PEMFC stack, and N_{fc} is the number of cells in series.

In this study, the PEMFC is configured with Matlab/Simulink Simscape library.

3) *Battery Model:* To balance the cost, energy density, power density, safety performance, and life span, Li-ion battery is the most applied battery type in marine ESS applications [27]. Simple models based on the equivalent circuit of a resistor in series with a parallel *RC* circuit (polarization circuit) [28] have been used to determine the dynamic characteristics of the battery, as shown in Fig. 4(b).

Open-circuit voltage (OCV) is defined differently for discharging and charging at given state-of-charge (SoC) due to the hysteresis effect [29]. The total voltage drop from OCV is then modeled here based on the first-order equivalent circuit to account for the internal resistance and polarization (OCV relaxation).

$$V_{\text{term}} = V_{\text{OCV}} - IR_e - V_p \tag{12}$$

where V_{term} is the terminal voltage of the cell, V_{OCV} is the cell OCV, I is the current rate of the cell (positive for discharging and negative for charging), R_e is the electrical resistance (responsible for instantaneous voltage drop together with C_p, after the application of load) and V_p is the voltage drop across the polarization circuit.

At any instant, V_p across the parallel *RC* circuit is represented by the voltage drop acrossR_p or C_p. So, the equation can be arranged by

$$\frac{V_p(t)}{R_p} + C_p \frac{dV_p(t)}{dt} = I(t) \tag{13}$$

where I_{Rp} is the current across polarization resistance, and I_{Cp} is the current across polarization capacitance. The sum of I_{Rp} and I_{Cp} gives the total circuit current I.

Then perform Laplace transform by

$$V_p(s) = I(s)\frac{R_p}{1 + sR_pC_p} \tag{14}$$

so that the steady-state response of terminal voltage $V_{\text{term } s-s}$ to a given current by

$$V_{\text{terms}-s} = V_{\text{OCV}} - I(R_e + R_p) = V_{\text{OCV}} - IR_{ti} \tag{15}$$

where $R_{ti} = R_e + R_p$ is the total internal resistance of a cell.

SoC is another critical parameter for the battery system. SoC is intrinsically divided into two types: Instantaneous SoC (SoC_{inst}) and nominal SoC (SoC_{nom}), both based on Ah counting. Nominal SoC is derived from nominal capacity based on standard discharging conditions as suggested by the manufacturer, while instantaneous SoC is based on the available instantaneous discharge capacity given by

$$\text{SoC}_{\text{nom}}(t_i) = \text{SoC}_{\text{nom}}(t_{i-1}) - \frac{I_{\text{step}}(t_{i-1})t_{\text{step}}}{C_{\text{nom}}} \tag{16}$$

$$\text{SoC}_{\text{inst}}(t_i) = \frac{(1 - \text{SoC}_{\text{nom}}(t_{i-1}))C_{\text{nom}}}{C_{\text{step avail}}(t_{i-1})} - \frac{I_{\text{step}}(t_{i-1})t_{\text{step}}}{C_{\text{step avail}}(t_{i-1})} \tag{17}$$

where, I_{step} is the current at a given time step, t_{step} is the span of time under consideration (sampling time of BMS/controller), and $C_{\text{step avail}}$ is the capacity available for I_{step}. Instantaneous SoC is useful in indicating the capacity available at a given time step and operating conditions, especially higher discharge rates.

In this study, the Matlab/Simulink Simscape battery stack model is utilized.

B. Power Electronic Converter Modeling

A dc/dc converter (for fuel cell and battery control), and an ac/dc rectifier (for diesel generator control) are modeled in this section.

1) *DC/DC Converter Model:* Both of the fuel cells and the battery systems are powered by dc/dc converter. The dc/dc converter regulates the output voltage and power flow from the storage device [8]. Different from the battery bidirectional control [31], fuel cells only require a single direction power flow to provide the power to dc link. It can be represented as the following equation:

$$\frac{V_{dc}}{V_{\text{ESS}}} = \frac{1}{1 - D} \tag{18}$$

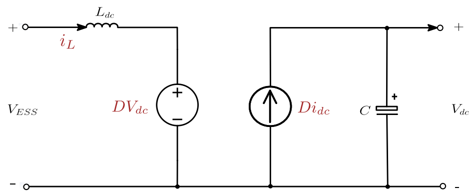

Fig. 5. DC/DC converter average model.

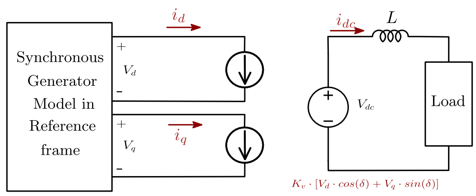

Fig. 6. Average model of 6-Pulse ac/dc rectifier, where V_d, V_q, I_d, I_q are generator's output voltage and current in $dq - axes$, δ is the angle between V_d and V_q, coefficient K_v is the ratio between the magnitude of rectifier output voltage V_{dc} and its input voltage V_d, V_q, and δ.

where D is the duty cycle of dc/dc converter.

There are two methods to model the power electronic converters, i.e., electromagnetic transient (EMT) model and average model. EMT model is straightforward and can represent the modulation process of the power electronic device. However, the simulation speed will be slow down due to the usage of high-frequency carriers during pulsewidth modulation (PWM). EMT simulation method is more suitable for system stability analysis studies, but not suitable to evaluate system performance throughout the operational profile which can last in the order minutes or even hours. For that reason, the average model is selected to configure the shipboard power plant model here. The dc/dc converter average model is shown in Fig. 5.

2) *AC/DC Rectifier Model:* The DGs are connected into dc bus via a 6-pulse diode rectifier. The average model of a diode bridge loaded synchronous generator was used here to simplify the calculation of the average values of generator *d-q* variables to the dc voltage and current at the bridge output [32], as shown in Fig. 6.

The voltage and current at the dc terminal can be defined as proportional to the amplitudes of the first harmonics of generator phase voltage and current, respectively [33]

$$V_{dc} = K_v \sqrt{V_d^2 + V_q^2} \tag{19}$$

$$i_{dc} = K_i \sqrt{i_d^2 + i_q^2} \tag{20}$$

where V_{dc} is dc voltage output from the rectifier. V_d, V_q, i_d, and i_d are the voltage and current of generator in *dq*-axes. K_v is the generator voltage constant, and K_i is the generator current constant.

C. System Control Philosophy

For existing hybrid shipboard power management is usually arranged in line with the hierarchical control framework. The basic structure is shown in Fig. 7.

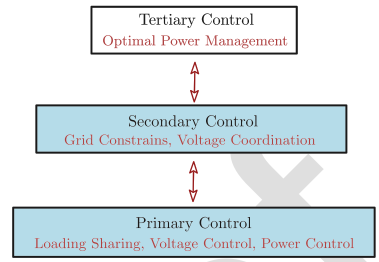

Fig. 7. Hierarchical control framework for shipboard power management, where the primary and secondary control have been applied.

In hierarchical control, the primary control level is to handle the load sharing among the hybrid power sources. The secondary control level includes the grid voltage coordination and to ensure bus signals at their operating ranges. The tertiary control level is used to achieve optimal operation with intentional objectives [34]. In this study, the primary and secondary level power management control have been achieved, while the tertiary control will be considered in future's research work.

The basic load sharing mechanism in dc-distributed power network is dc voltage droop control. Basically, with the voltage droop control, all the power sources share the load based on the dc bus voltage in the similar way as with frequency droop control in ac-distributed system. The load sharing function is realized by adjusting the voltage droop rate. In Fig. 8, it shows the load sharing results of a dc power network with three different droop rate setting. A steeper droop angle will cause one consumer to take less load than one with a more flat droop angle given the same voltage set point.

DG system is integrated into the dc network via 6-pulse diode rectifier, and the output voltage is controlled by AVR. The dc voltage set point is defined as the nominal dc voltage of the rectifier. Droop increases with increasing generator speed. Usually, the dc voltage droop rate is not larger than 5% [35].

For the energy storage power sources, such as fuel cells and batteries, the dc voltage droop control is implemented in the power electronic dc/dc converters. The block diagram of the voltage control loop is as shown in Fig. 9. It is a dual control loop, with the current control as the inner loop with the voltage control as the outer loop. $K_{dr,v}$ is the voltage droop rate for load sharing with other power sources.

The dc voltage droop control is simple and reliable. But due to the complexity of hybrid dc-grid system configuration, it is difficult to fine-tune the whole power system with one single parameter to maintain the performance of each power source, and ensure the system stability at the same time. It is also not possible to achieve strategy loading or even optimized operation. Therefore, the power control of the ESS devices is expected. The dc/dc converter power control loop with PI controllers is shown in Fig. 10. It is a single current control loop, where the current reference is given by the quotient of reference power and dc voltage.

In this study, dc voltage droop combined with power control is implemented as primary power management scheme. The system voltage coordination rules and constrains have been set in power electronic converter models as the secondary level of

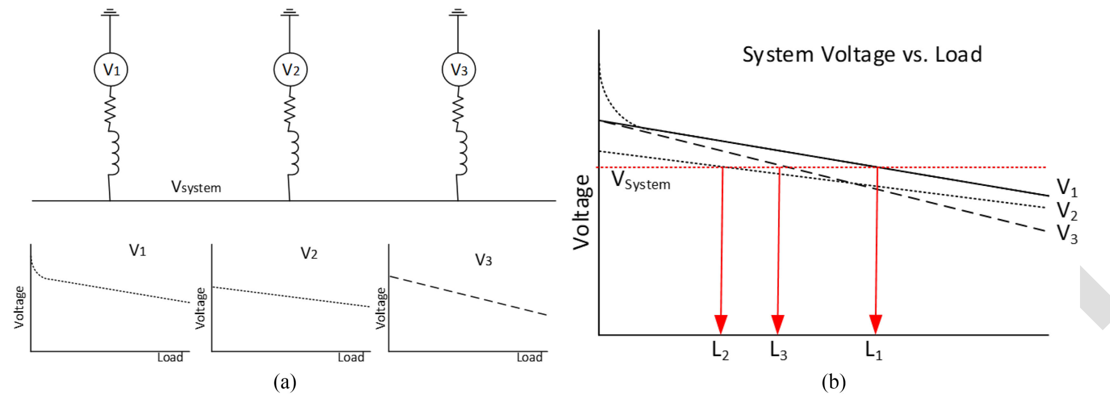

Fig. 8. Load sharing with 3 different droop curves. (a) Integrated dc-distributed system with three power sources and their droop rates. (b) System voltage and load sharing scheme.

TABLE I
PARAMETERS FOR THE DC-BASED DEMO VESSEL

Diesel-generator		**Fuel cell [30]**		**Batteries**	
Rated power (P_{gen})	410 kW	Rated power (P_{fc})	2*100 kW	Capacity (E_{batt})	113 kWh
Nominal voltage (V_{abc})	400 VAC	Min. power (P_{fc_min})	20 kW	Max. charge voltage (V_{batt_max})	350VDC
Nominal current (I_{abc})	592 A	Operating voltage (V_{fc})	355-577 VDC	Nominal voltage (V_{batt})	300 VDC
Frequency (F_n)	50 Hz	Rated current (I_{fc})	2*257 A	Min. voltage (V_{batt_min})	268 VDC
Speed (Spd)	1500 rpm	Max. Temperature (T_{max})	70°C	Max. discharge current (I_{batt_disch})	250 A
Inertia (J_{ge})	10 kgm^2	Fuel Type	Hydrogen	Max. charge current (I_{batt_ch})	200 A
Power factor (pf)	0.9	H_2 pressure	3.5-5 Barg	Operating state of charge range (SoC)	20%-80%

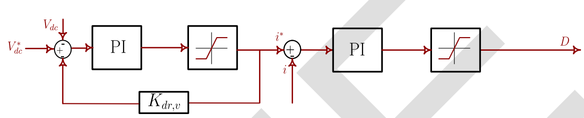

Fig. 9. DC/DC converter control scheme I - Voltage control loop.

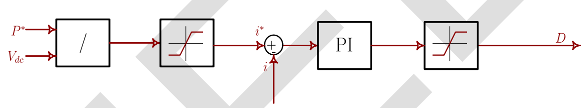

Fig. 10. DC/DC converter control scheme II - Power control loop.

power management.The ESS device output power or voltage shall be regulated according to the reference command if the corresponding control scheme is selected. Two different operation modes will be studied in this article: Zero-emission mode and DG in-parallel mode.

D. System Simulation Results

A small-scaled tugboat power plant is configured as the target vessel for simulation test. It is a typical hybrid shipboard dc-grid system design, as shown in Fig. 2. It comprises two sets of 200-kW fuel cells, two battery arrays with capacity of 113 kWh and two 410-kW DGs as the back-up power. The detailed system configuration parameters for this dc-based demo vessel are shown in Table I. The simulation tests are performed with two operating modes, respectively: Zero-emission mode and DG in-parallel mode. The test results are shown as follows.

1) *Zero-Emission Mode:* During the zero-emission mode operation, there is no DG online. The battery units are working under the voltage control scheme to regulate the system dc-grid voltage level. Two battery sets share the load via voltage droop control. Fig. 11 shows the simulation results for the dc-grid hybrid power plant performance under zero-emission operation.

a) $T = 3$*–15 s*: The load power increases to 300 kW. The total load demands are supplied by two fuel cell modules and two battery units. Fuel cells follow the power references from the dc/dc converter, while batteries share the remaining required power equally when the voltage droop rate is set as the same value. In this test, voltage droop rate is set as 3%.

b) $T = 15$*–30 s*: The propulsion load is dropped. The batteries switch to charging mode to absorb the remaining power from network for future usage.

c) $T = 30$ *s–end*: the load is increased to peak, around 400 kW. The batteries discharge and provide the power supply for the peak load demands.

It shows that the dynamic response of fuel cells is relatively slow and it needs the battery systems' support to fulfill the peak ship load. With voltage droop control, the system dc voltage slightly varies according to the different loading conditions. Two fuel cells are operated independently according to their own reference profiles. Usually in real practice, fuel cells can be set to provide the average load demands [36], and the batteries are to enhance the system dynamic performance and boost the power supply during peak load.

2) *DG in-Parallel Mode:* When the system is under DG in parallel mode, the DGs connect to dc network via a

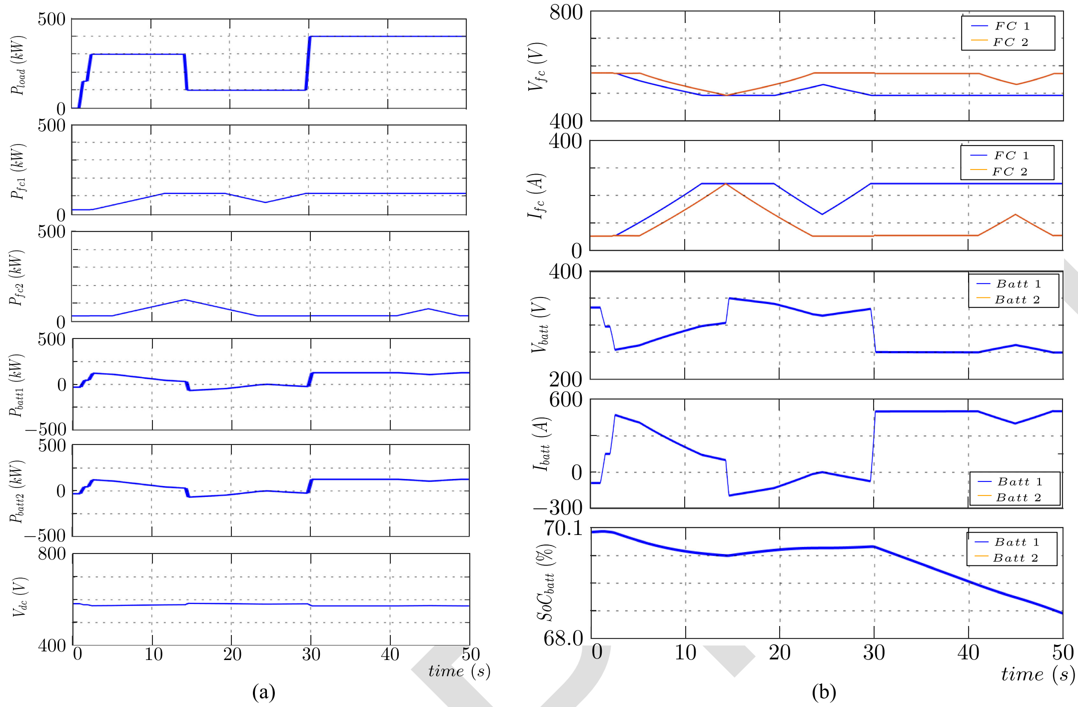

Fig. 11. Simulation results for the dc-based shipboard power grid model for demo vessel. Zero-emission mode. (a) Power split of the hybrid shipboard power plant model. (b) Dynamic behavior of fuel cell devices and batteries.

6-pulsed passive rectifier. The online diesel generators dominate the system dc voltage level naturally by its terminal ac voltage. In this case, battery systems are switched to power control scheme which is similar to the fuel cell control method to provide the output power flow as reference required to achieve an ideal loading strategy and optimization control. Fig. 12 shows the simulation results of the hybrid ship power system under DG in-parallel mode.

a) *T* = *3 - 15 s*: The load power increases to peak 400 kW. The fuel cell modules follow the power reference commands from the dc/dc converter. The propulsion load variations are absorbed and equally shared between two battery units. The voltage droop rate here is set as 2% for both the DGs so that they are able to share equal 100-kW load throughout the simulation.
b) *T* = *15 - 30 s*: The propulsion load is dropped. The batteries switch to charging mode to absorb the extra power for future usage.
c) *T* = *30 s - end*: The power of the load is shooting up to the peak again. The batteries discharge and boost the total power supply.

In this simulation test, fuel cells and battery systems provide the power supply according to the power allocation reference, and the remaining power demands from the network go to DGs online. Similar to the zero-emission mode, the batteries function as the dynamic enhancement to support the system dynamic performance. To maintain system stability, the generators shall remain stable outputs, and usually, it can be set as the average load demands.

For both zero-emission mode and DG in-parallel mode simulation test, the different power sources are integrated into the common dc-distributed power network and able to satisfy the load demands. The system power load sharing is under dc voltage droop combined with power control scheme. During both of the operation modes, the power reference profile for the two fuel cells are set differently. This system-level hybrid power plant model provides the control freedom to interface with different tertiary level power management algorithms.

IV. HIL Setup

Control algorithm testing can be time-consuming, costly, and potentially unsafe if the test is against a real hardware-based system. Therefore, software-based plant model is considered for replacing the real system and to generate the operational profile of a vessel. A HIL setup is expected to provide real-time simulation of the shipboard power system behavior and dynamics, as well as the hardwired interfaces with control signals and communication protocols. HIL test is able to ensure high quality of the control software. It is a reliable verification and validation method to prototype the controller before implementing the control algorithm into a real hardware environment [37].

In this study, the shipboard power system plant model is successfully built and run on a real-time Speedgoat target machine, which provides real-time simulation of plant model behavior and dynamics as well as the communication interface with field-bus protocols. The power and energy optimization control algorithms are developed and downloaded to a B&R brand X20CP3586 programmable logic controller (PLC)-based

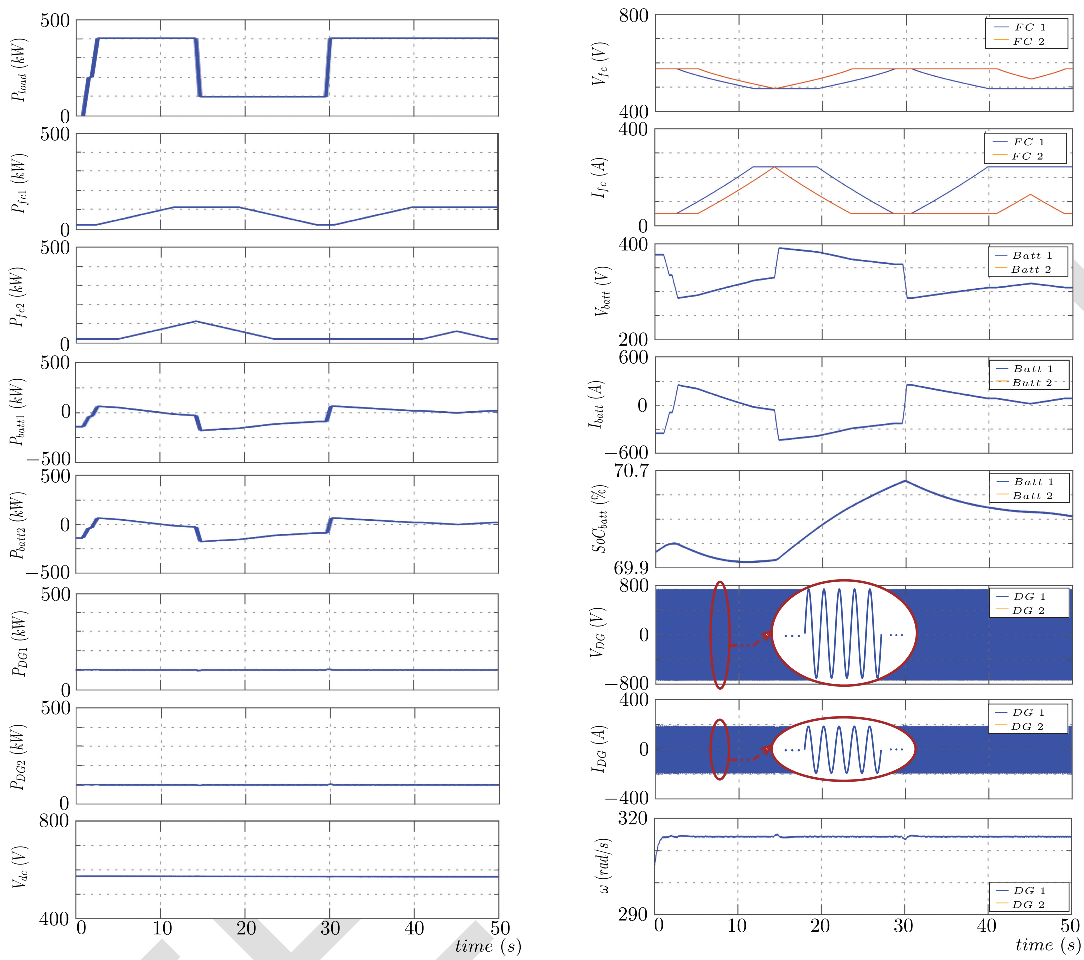

(a) (b)

Fig. 12. Simulation results for the dc-based shipboard power grid model for demo vessel. DG in-parallel mode. Frequency of the DG is 50 Hz. (a) Power split of the hybrid shipboard power plant model. (b) Dynamic behavior of fuel cell devices, batteries and DGs.

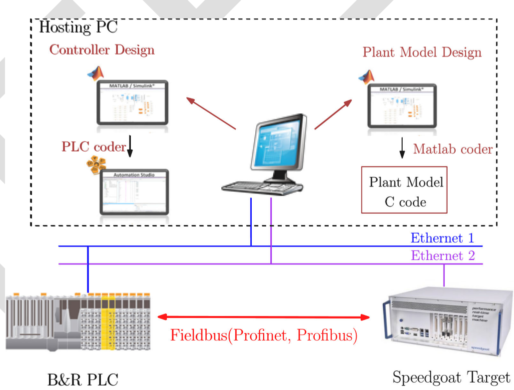

Fig. 13. HIL topology scheme.

embedded control system. The available real-time Fieldbus communication protocols between the plant model and controller are Profinet and Profibus for this setup. In this study, the topology diagram of the HIL test bed is shown in Fig. 13.

V. System Model Validation

In this study, the mathematical shipboard power system model and HIL plant are both validated against the full-scale hybrid power plant system. The actual power grid facilities are located at ABB collaborated hybrid power laboratory in MARINTEK, at Norwegian University of Science and Technology, in Trondheim, Norway. The main objective of this experimental validation test is to verify that the response of the modeled shipboard power system matches with the actual system response. The DGs and fuel cells with battery energy storage will be validated, respectively, according to the actual lab setup.

The system configuration of the MARINTEK laboratory is based on a full-scale hybrid AES with ABB onboard dc-grid system. The lab arrangement diagram is shown in Fig. 14. The lab is equipped with two 410-kW diesel engines and variable speed generator sets, two 30-kW fuel cell devices, plus one 55-kWh battery ESS. Power sources are connected to the dc-bus, and system loading conditions are simulated with two controllable electric motors. Fig. 15 shows the equipment setup in MARINTEK lab.

In the first validation test, one DG and one 55-kWh battery system are in use. The validation test results are shown in Fig. 16. The load profile is designed as four ramp-up cycles The dynamic response of a DG is limited by its mechanical characteristic, and so the battery banks are there to boost the system dynamic performance to achieve the load demands. In this test, the

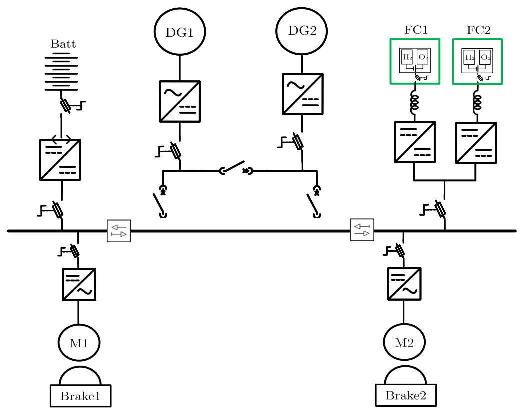

Fig. 14. ABB MARINTEK lab setup diagram, where M1 & M2 are the propulsion motors, and Brake1 & 2 present the controllable thrusters load.

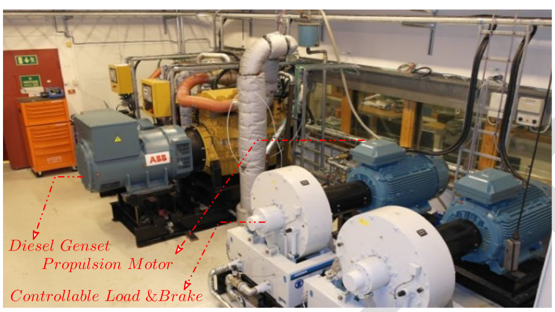

Fig. 15. ABB MARINTEK lab in Trondheim, Norway.

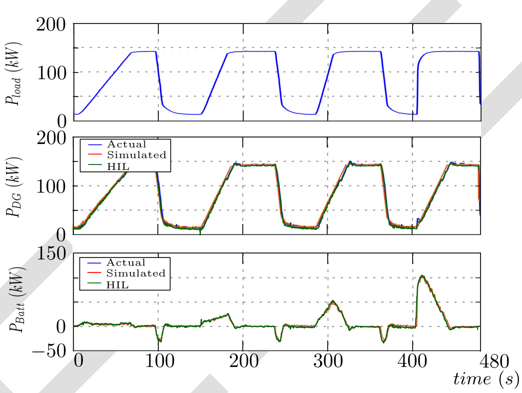

Fig. 16. Validation test I: To compare the system response between simulation model and HIL plant target in DG in-parallel mode.

simulated results from the Simulink model can match well with the actual recorded test. The overall mean average percentage error between the mathematical plant model and actual system is around 0.51%, and the average error between HIL plant and actual system is about 1.82%.

In the second validation test, two fuel cell modules and the same battery system are configured. The test results are shown in Fig. 17. During the first 100 s, the two fuel cells were powered up with 9-kW output one after another. The power drawn from the batteries was reduced with the increasing power supply from the fuel cells. From the 120 s, the load demands are reduced below the fuel cell power supply so that the batteries are charged by the fuel cells. Between 100 to 480 s, the fuel cells provide the constant power output, while the batteries absorb the load

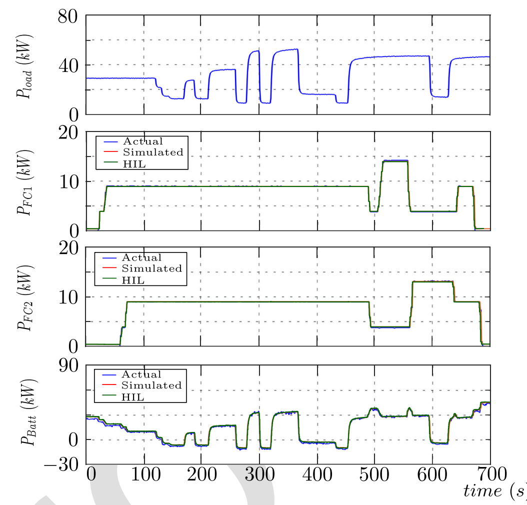

Fig. 17. Validation test II: To compare the system response between simulation model and HIL plant target in Zero-emission mode.

variations. From the 480 s onward, the power references for fuel cells are altered so that the batteries provide the remaining power to the load. The mean average percentage error is about 1.98% between the mathematical model and the actual system, while it is about 1.47% between HIL plant and the actual system.

To compare the test results, it can be seen that the system simulation and HIL results compare well with the experimental values recorded from the site. In addition, the transient rise time and steady-state power output for all DG, fuel cells, and battery power sources for both mathematical model and HIL plant can be in line with the actual system responses. Therefore, the proposed hybrid shipboard power plant model can be used to represent the physical system behavior.

VI. Conclusion

In this article, adc-distributed hybrid shipboard power system configuration has been studied. A system-level fuel cell-fed hybrid shipboard power grid system with dc distribution has been modeled. In addition, an HIL plant model platform has been set up and tested in a lab environment. Finally, both the system mathematical model and the HIL plant have been validated against a full-scale hybrid shipboard power system. This research work provides an essential platform and solid foundation to apply optimization control of power and energy management strategy in future work.

Acknowledgment

The authors would like to thank Dr. J.-F. Hansen, Dr. S. Kanerva, and their team for sharing their expertise and support to access the lab facility and data.

References

[1] *Review of Maritime Transport*, United Nations Conf. Trade Develop., Geneva, Switzerland, No. UNCTAD/RMT/2011, 2011.

[2] MARPOL, "International convention for the prevention of pollution from ships," 2019. [Online]. Available: http://www.mar.ist.utl.pt/mventura/Projecto-Navios-I/IMO-Conventions%20%28copies%29/MARPOL.pdf

[3] E. Hughes, "Initial IMO strategy on reduction of GHG emissions from ships," Int. Maritime Org., London, U.K., 2018.

[4] R. Ashdown, "The shipboard energy efficiency management plan (SEEMP)," in *Proc. IACS-EU Maritime Transp. Workshop*, 2017, pp. 2–7.

[5] C. Nuchturee and T. Li, "A review of energy efficient methods for all-electric ships," *IOP Conf. Series, Earth Environ. Sci.*, vol. 188, 2018, Art. no. 012050.

[6] P. Lin, T. Zhao, B. Wang, Y. Wang, and P. Wang, "A semi-consensus strategy toward multi-functional hybrid energy storage system in dc microgrids," *IEEE Trans. Energy Convers.*, vol. 35, no. 1, pp. 2787–2793, Mar. 2020.

[7] R. T. Amin, A. S. Bambang, C. J. Rohman, R. Dronkers Ortega, and A. Sasongko, "Energy management of fuel cell/battery/supercapacitor hybrid power sources using model predictive control," *IEEE Trans. Ind. Informat.*, vol. 10, no. 4, pp. 1992–2002, Nov. 2014.

[8] L. W. Y. Chua, "Power management for all-electric hybrid marine power systems," Ph.D. dissertation, School Mech. Aerosp. Eng. (MAE), Nanyang Technol. Uni., Singapore, 2018.

[9] J. Chen, L. Huang, C. Yan, and Z. Liu, "A dynamic scalable segmented model of PEM fuel cell systems with two-phase water flow," *Math. Comput. Simul.*, vol. 167, pp. 48–64, 2018.

[10] D. Stapersma and H. K. Woud, *Design of Propulsion and Electric Power Generation System*. London, U.K., IMarEST, 2002.

[11] R. E. Hebner *et al.*, "Technical cross-fertilization between terrestrial microgrids and ship power systems," *J. Modern Power Syst. Clean Energy*, vol. 4, no. 2, pp. 161–179, Apr. 2016.

[12] S. Fang, Y. Wang, B. Gou, and Y. Xu, "Toward future green maritime transportation: An overview of seaport microgrids and all-electric ships," *IEEE Trans. Veh. Technol.*, vol. 69, no. 1, pp. 207–219, Jan. 2020.

[13] W. Chen *et al.*, "On the modelling of fuel cell-fed power system in electrified vessels," in *Proc. IEEE 21st Workshop Control Model. Power Electron.*, 2020, pp. 1–8.

[14] M. Al-falahi, T. Tarasiuk, S. Jayasinghe, Z. Jin, H. Enshaei, and J. Guerrero, "Microgrids: Control and power management optimization," *Energies*, vol. 11, 2018, Art. no. 1458.

[15] Z. Jin, L. Meng, J. M. Guerrero, and R. Han, "Hierarchical control design for a shipboard power system with dc distribution and energy storage aboard future more-electric ships," *IEEE Trans. Ind. Informat.*, vol. 14, no. 2, pp. 703–714, Feb. 2018.

[16] P. W. Tomislav Dragicevic and F. Blaabjerg, *DC Distribution Systems and Microgrids*. London, U.K.: Inst. Eng. Technol., 2018.

[17] A. Haxhiu, A. Abdelhakim, S. Kanerva, and J. Bogen, "Electric power integration schemes of the hybrid fuel cells and batteries-fed marine vessels—An overview," *IEEE Trans. Transport. Electrific.*, to be published, doi: 10.1109/TTE.2021.3126100.

[18] J. P. Trovão, F. Machado, and P. G. Pereirinha, "Hybrid electric excursion ships power supply system based on a multiple energy storage system," *IET Elect. Syst. Transp.*, vol. 6, no. 3, pp. 190–201, 2016.

[19] "Onboard DC grid: The step forward in power generation and propulsion," ABB AS, Billingstad, Norway, 2013.

[20] *IEEE Recommended Practice for Excitation System Models for Power System Stability Studies*, IEEE Standard 421.5–2016 (Revision of IEEE Std 421.5-2005), 2016.

[21] S. Roy, O. P. Malik, and G. S. Hope, "A low order computer model for adaptive speed control of diesel driven power-plants," in *Proc. Conf. Rec. IEEE Ind. Appl. Soc. Annu. Meeting*, 1991, pp. 1636–1642.

[22] M. A. Rahman, A. M. Osheiba, T. S. Radwan, and E. S. Abdin, "Modelling and controller design of an isolated diesel engine permanent magnet synchronous generator," *IEEE Trans. Energy Convers.*, vol. 11, no. 2, pp. 324–330, Jun. 1996.

[23] T. Tronstad, H. H. Åstrand, G. P. Haugom, and L. Langfeldt, "DNV-GL EMSA study on the use of fuel cells in shipping," EMSA European Maritime Safety Agency, 2017. [Online]. Available: https://www.studocu.com/en-gb/document/brunel-university-london/energy-conversion-technologies/emsa-study-on-the-use-of-fuel-cells-in-shipping/5956606

[24] L. Kong, J. Yu, and G. Cai, "Modeling, control and simulation of a photovoltaic/hydrogen/supercapacitor hybrid power generation system for grid-connected application," *Int. J. Hydrogen Energy*, vol. 44, no. 46, pp. 25129–25144, 2019.

[25] M. İnci, M. Büyük, M. M. Savrun, and M. H. Demir, "Design and analysis of fuel cell vehicle-to-grid (FCV2G) system with high voltage conversion interface for sustainable energy production," *Sustain. Cities Soc.*, vol. 67, 2021, Art. no. 102753.

[26] M. M. Savrun and M. İnci, "Adaptive neuro-fuzzy inference system combined with genetic algorithm to improve power extraction capability in fuel cell applications," *J. Cleaner Prod.*, vol. 299, 2021, Art. no. 126944.

[27] B. Perry, "High capacity battery packs," ABB Generation, white paper, 2019. [Online]. Available: https://library.e.abb.com/public/82b8e284d5fdc935c1257a8a003c26a4/ABB%20Generations_22%20High%20capacity%20battery%20packs.pdf

[28] J. Gao, S.-Q. Shi, and H. Li, "Brief overview of electrochemical potential in lithium ion batteries," *Chin. Phys. B*, vol. 25, no. 1, Jan. 2016, Art. no. 018210.

[29] M. Farag, "Lithium-ion batteries: Modelling and state of charge estimation," Ph.D. dissertation, Dept. Mech. Eng., McMaster Univ., Hamilton, ON, Canada, 2013.

[30] "PEM fuel cell module for heavy duty motive applications–Product data sheet," Ballard, Burnaby, BC, Canada, 2018. [Online]. Available: https://hfcnexus.com/wp-content/uploads/2016/07/Ballard-FCmove-data-sheet.pdf

[31] W. Chen, A. K. Ådnanses, J. F. Hansen, J. O. Lindtjørn, and T. Tang, "Super-capacitors based hybrid converter in marine electric propulsion system," in *Proc. 19th Int. Conf. Elect. Mach.*, 2010, pp. 1–6.

[32] H. Zhu, "New multi-pulse diode rectifier average models for AC and DC power systems studies," Ph.D. dissertation, Bradley Elect. Comput. Eng. Dept., Virginia Polytech. Inst. State Univ., Blacksburg, VA, USA, 2005.

[33] I. Jadric, D. Borojevic, and M. Jadric, "A simplified model of a variable speed synchronous generator loaded with diode rectifier," in *Proc. Rec. 28th Annu. IEEE Power Electron. Specialists Conf., Formerly Power Conditioning Specialists Conf. Power Process. Electron. Specialists Conf.*, 1997, vol. 1, pp. 497–502.

[34] J. M. Guerrero, J. C. Vasquez, J. Matas, L. G. de Vicuna, and M. Castilla, "Hierarchical control of droop-controlled AC and DC microgrids-A general approach toward standardization," *IEEE Trans. Ind. Electron.*, vol. 58, no. 1, pp. 158–172, Jan. 2011.

[35] F. Thams, S. Chatzivasileiadis, and R. Eriksson, "DC voltage droop control structures and its impact on the interaction modes in interconnected AC-HVDC systems," in *Proc. IEEE Innov. Smart Grid Technol. - Asia Proc. IEEE Innov. Smart Grid Technol.- Asia*, 2017, pp. 1–6.

[36] A. Rabbani, "Dynamic performance of a PEM fuel cell system," Ph.D. dissertation, Tech. Univ. Denmark, Kongens Lyngby, Denmark, 2019.

[37] D. J. Murray-Smith, "Real-time simulation, virtual prototyping and partial-system testing," in *Modelling and Simulation of Integrated Systems in Engineering*. Sawston, U.K.: Woodhead, 2012.

Wenjie Chen (Student Member, IEEE) received the B.Sc. degree in automation from Shanghai Maritime University, Shanghai, China, in 2007, the M.Sc. degrees in electrical engineering from Ecole Polytechnique de l'Université de Nantes, France, in 2009. She is currently working toward the Ph.D. degree in optimization control for power system under the supervision of Prof. K. Tai with Nanyang Technological University, Singapore, and Prof. T. Tjahjowidodo with Katholieke Universiteit Leuven, Leuven, Belgium, since January 2019.

She firstly joined ABB China (Shanghai) in 2010, and then transferred to ABB Singapore in 2011. Currently, she is based in Singapore as a Research Specialist.

Kang Tai received the B.Eng. degree in mechanical engineering from the National University of Singapore, Singapore, and the Ph.D. degree from Imperial College, London, U.K.

He is currently an Associate Professor with the School of Mechanical and Aerospace Engineering, Nanyang Technological University, Singapore. His research interests include optimization, evolutionary computation, mathematical/empirical modeling of industrial processes, and analysis of interdependencies, risks and vulnerabilities in critical infrastructure networks.

Michael Lau received the Ph.D. degree in mechanical engineering from Aston University, Aston, U.K. and the C.Eng. degree from Institution of Mechanical Engineers, London, U.K.

He was a Control and Instrument Engineer with Ministry of Defence, Singapore, and later with an oil and gas industry for about four years, before spending the next 35 years as an academician, first with Nanyang Technological University, Singapore, until 2010, and then with Newcastle University in Singapore (NUiS), Singapore till current. He is currently an Associate Professor with NUiS. His research interests include control, mechatronics system designs and energy systems.

Ahmed Abdelhakim (Senior Member, IEEE) was born in Egypt on April 1, 1990. He received the B.Sc. and the M.Sc. degrees (with hons.) in electrical engineering from Alexandria University, Alexandria, Egypt, in 2011 and 2013 respectively, and the Ph.D. degree from the University of Padova, Vicenza, Italy, in 2019.

He is currently with ABB Research Sweden as a Principal Scientist Scientist and R&D Project Manager. His research interests include power electronics converters and their applications for fuel cells and energy storage systems, investigation of new power converter topologies, and application of wide-bandgap semiconductor devices (GaN/SiC) for high frequency and high-power density power converters.

Dr. Abdelhakim was the recipient of the classified excellent Ph.D. dissertation award from Societá Italiana di Electronica (SIE'19) among Italian Universities, in 2019. He serves as an Associate Editor for the IEEE TRANSACTION ON INDUSTRIAL ELECTRONICS and IEEE TRANSACTION ON TRANSPORTATION ELECTRIFICATION.

Ricky R. Chan received the Ph.D. degree in electrical engineering from Purdue University, West Lafayette, IN, USA, in 2009.

He is currently a Research and Development Manager with ABB Marine & Ports in Helsinki, Finland, where he leads a team of specialists in the development of advanced electric solutions for marine applications.

Alf Kåre Ådnanes received the M.Sc. and Ph.D. degrees in electrical engineering from the Norwegian University of Science and Technology, Trondheim, Norway.

He heads the regional division in AMEA of ABB Marine & Ports. He joined ABB in 1991, and among previous positions with ABB, he has worked within corporate research, and various positions within Marine, including delivery projects, engineering, and in product management and development, and technology management for the global marine business unit for Marine & Ports.

Tegoeh Tjahjowidodo received the Ph.D. degree in mechanical engineering and automation from KU Leuven, Belgium in 2006.

He is currently an Associate Professor with the Department of Mechanical Engineering, KU Leuven. From 2009 until 2019, he has been with the School of Mechanical & Aerospace Engineering, Nanyang Technological University, Singapore, as an Associate Professor. His research interests include nonlinear dynamics, modeling, identification and control, with more focus in monitoring for manufacturing.

DC-Distributed Power System Modeling and Hardware-in-the-Loop (HIL) Evaluation of Fuel Cell-Powered Marine Vessel

Wenjie Chen, *Student Member, IEEE*, Kang Tai, Michael Lau, Ahmed Abdelhakim, *Senior Member, IEEE*, Ricky R. Chan, Alf Kåre Ådnanes, and Tegoeh Tjahjowidodo

***Abstract*—Environmentally driven regulations are significantly affecting shipping in recent years, where the shipbuilding industry is required to comply with upcoming restrictions concerning polluting emissions. The all-electric ship (AES) is one of the most promising technologies for complying with the increasingly strict environmental regulations, improving fuel efficiency, and enhancing system dynamic performance. In this study, the dc-distributed power grid of an AES integrated with fuel cells and batteries has been configured using extensive electrification technology, where the system-level shipboard power plant has been modeled with the average modeling method. The model not only incorporates the hybrid power source integration but also the primary and secondary power management as a whole. In addition, a hardware-in-the-loop (HIL) has been set up to replicate the real-time system behavior, which is essential for the verification of any optimal power management control algorithms to be developed in future work. Finally, both the mathematical and real-time models are validated against the full-scale hybrid shipboard power system.**

***Index Terms*—All-electric ship, fuel cell system (AES), hardware-in-the-loop (HIL), hybrid shipboard power microgrid, renewable energy sources.**

I. Introduction

MARITIME transport has played a dominant role in the global trade system for centuries, and it is expected that international maritime trade will expand at continuous annual growth for years to come [1]. Recently, environmental sustainability has become a significant policy concern in global maritime transport [2]. With this concern, the shipbuilding industries are compelled to abide by rules on polluting emissions imposed by International Maritime Organization (IMO) and national legislation [3]. To achieve high energy efficiency and low emission, it is believed that the all-electric ship (AES) will be one of the most promising technologies to comply with the environmental regulations [4]. In particular, vessel types such as tug boats, river pushers, and ferries will be the early adopters as they usually operate near coasts or in inner rivers, which belong to emission control areas (ECAs). Other vessel types such as container vessels may need more time before the AES design can be adopted [5].

With the development of energy storage technologies, new energy sources can be integrated into the shipboard power network. Batteries, as the most mature energy storage system (ESS) device, have been widely utilized in different applications in marine vessels. However, due to energy density limitation, battery systems only function as a main power supply for small-scale vessels in short distance shipping segment or as an auxiliary power source onboard of large vessels to enhance the dynamic performance or short-term zero-emission operation. In order for clean energy sources to be a feasible solution for larger ocean-going ship types, such as cruise ships and RoRo/RoPax (the vessels built for freight vehicle transport with passenger accommodation), fuel cell systems have been introduced. It is expected that fuel cell systems would replace diesel engines as the main power source in the future.

The hybrid shipboard power system integrated with different types of power sources brings in a lot of benefits, but it also increases the complexity of the system structure and power management control. To get deep understanding of the hybrid power system and improve the current control algorithms, a comprehensive system-level hybrid power plant model is needed as a foundation. The expected system model should be able to perform the actual shipboard power plant responses under different operating modes and loading profiles.

A few power system configurations and modeling methodologies have been published in the recent literature. In [6] and [7], land-based hybrid dc microgrid configurations have

Manuscript received August 9, 2021; revised October 25, 2021, December 13, 2021, and December 17, 2021; accepted December 19, 2021. This work was supported in part by the Singapore Economic Development Board and ABB Pte. Ltd. Joint Industrial Postgraduate Program. *(Corresponding author: Wenjie Chen.)*

Wenjie Chen is with the School of Mechanical and Aerospace Engineering, Nanyang Technological University, Singapore 639798, and also with the ABB Pte. Ltd., Singapore 139935 (e-mail: wenjie003@e.ntu.edu.sg).

Kang Tai is with the School of Mechanical, and Aerospace Engineering, Nanyang Technological University, Singapore 639798 (e-mail: mktai@ntu.edu.sg).

Michael Lau is with the Newcastle University in Singapore, Singapore 599493 (e-mail: michael.lau@newcastle.ac.uk).

Ahmed Abdelhakim is with the ABB Corporate Research, 722 26 Västerås, Sweden (e-mail: ahmed.abdelhakim@se.abb.com).

Ricky R. Chan is with the Marine and Ports, ABB Oy, 1 00980 Helsinki, Finland (e-mail: ricky.chan@fi.abb.com).

Alf Kåre Ådnanes is with the Marine and Ports, ABB Engineering (Shanghai) Ltd., Shanghai 1 00980, China (e-mail: alfkare.adnanes@cn.abb.com).

Tegoeh Tjahjowidodo is with the Department of Mechanical Engineering, KU Leuven, De Nayer Campus, 2860 Sint-Katelijne-Waver, Belgium (e-mail: tegoeh.tjahjowidodo@kuleuven.be).

Color versions of one or more figures in this article are available at https://doi.org/10.1109/JESTIE.2021.3139471.

Digital Object Identifier 10.1109/JESTIE.2021.3139471

been introduced. The authors in [8] have proposed a diesel-generator-based marine power network equipped with a battery ESS, while a fuel cell-based marine system model has been developed in [9], where the authors are mainly focusing on the fuel cell chemical reaction and fuel processing. The above references focus only on certain parts of the power grid rather than the observation of the dynamics and performance of the complete system.

It is worth noting that shipboard power systems have their own special configurations and requirements [10]. The main difference with land-based power system is that shipboard power system is an isolated microgrid with short distances from generated power to the electric propulsion load [11]. The average short-circuit levels and forces are quite high so that it must be dealt with some special manners to protect the power equipment. During cruising, shipboard power system is impacted a lot by the environment, such as marine weather and unexpected thrusters load variations, therefore the system stability and reliability is crucial for marine vessels. Extra efforts in system reconfigurability and redundancy are required to prevent single point failure according to the marine classification rules. Compared to EV power system, the power scale of the shipboard power network is much bigger and complicated. Due to its particularity of the shipboard power system [12], there is the urge to build its own power plant model rather than reusing other existing models.

In addition, system-level power plant model is not only to integrate different power sources but also to implement primary and secondary level power management to coordinate power load sharing, frequency, and voltage control. A previous work by the authors [13] modeled an ac-distributed shipboard hybrid power system. However, in the past decade, dc-based distribution systems have gained popularity due to their advantages in many aspects [14]. A system-level dc-based shipboard power model is necessary to simulate the vessel operating performances. The comprehensive and reliable power plant model is the foundation and precondition for system studies and further research.

Compared to the existing studies on hybrid power network modeling problems, the main contributions of this article are highlighted as follows.

1) A dc-distributed system-level shipboard power system model is built, integrating the mathematical model of different power sources, as well as the primary and secondary power management control. All the power sources are resizable to configure the new shipboard systems according to the varied ship design specifications.
2) A hardware-in-the-loop (HIL) platform is set up in lab environment as well. HIL helps to perform the system real-time states. It is a useful tool for prototyping the power and energy management system (PEMS) controller and communication interface validation without involving any hardware devices setup.
3) Both the mathematical and real-time HIL model have been validated against the real hardware full-scale hybrid shipboard power system.

The rest of this article is organized as follows: The hybrid shipboard power system configuration is discussed in Section II. A dc-based power distribution model and the simulation results are presented in Section III. Section IV evaluates the system plant model HIL setup. And the validation tests are performed in Section V. Finally, Section VI concludes this article.

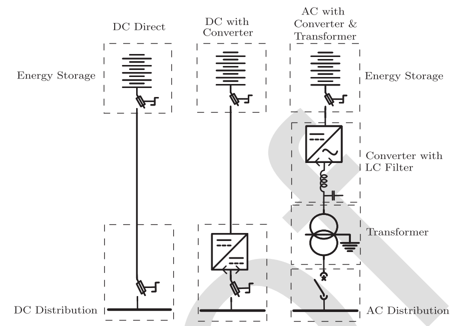

Fig. 1. ESS integration scheme for both dc and ac distribution system.

II. Shipboard Power System Configuration

In this section, the functions of several integration schemes will be introduced in detail. The advantages and the system configuration of dc-distributed shipboard power system will also be discussed.

A. *Advantages of DC-Based Shipboard Power System*

Currently, the majority of commercial marine vessels have a diesel or gas engine powered plant with ac distribution, while the dc-distributed shipboard system has drawn much attention over the past decade. In both ac and dc-distributed systems, ESS integration is a trend for different functionalities [15].

Energy storage, such as batteries will help the slow power devices level out load variations from the thrusters and other heavy consumers. Besides, the clean energy sources are able to provide the main power supply of the ship operation in order to achieve zero-emission operation. There are several methods to integrate the ESS into the shipboard network [16], which is shown in Fig. 1.

According to this integration scheme, it can be seen that the ESS is much easier to connect to a dc-distributed network than an ac system. The storage devices can be directly connected to the dc network. This direct-on-line (DOL) ESS gives an efficiency increase compared to the ESS with dc/dc converter, but at the cost of less control features to be achieved. On the other hand, ESS is also possible to be extended to an ac-distributed system through a dc/ac converter with LCL filter and transformer [17]. The *LCL* filter is used herein to improve the power quality and reduce the total harmonic distortion (THD) level of the main power network. While the shielded transformer is utilized to solve the electromagnetic interference (EMI) issue, it also blocks the circulating current within the power electronic converters such as IGBT or MOSFET. In addition, the dc/ac converters also need to monitor the amplitude, frequency, and phase shift of the power network voltage on ac side to achieve the synchronization operation [13]. It is clear that the ac-based power configuration is quite complex not only in system configuration but also in power management control [14]. Furthermore, it also increases

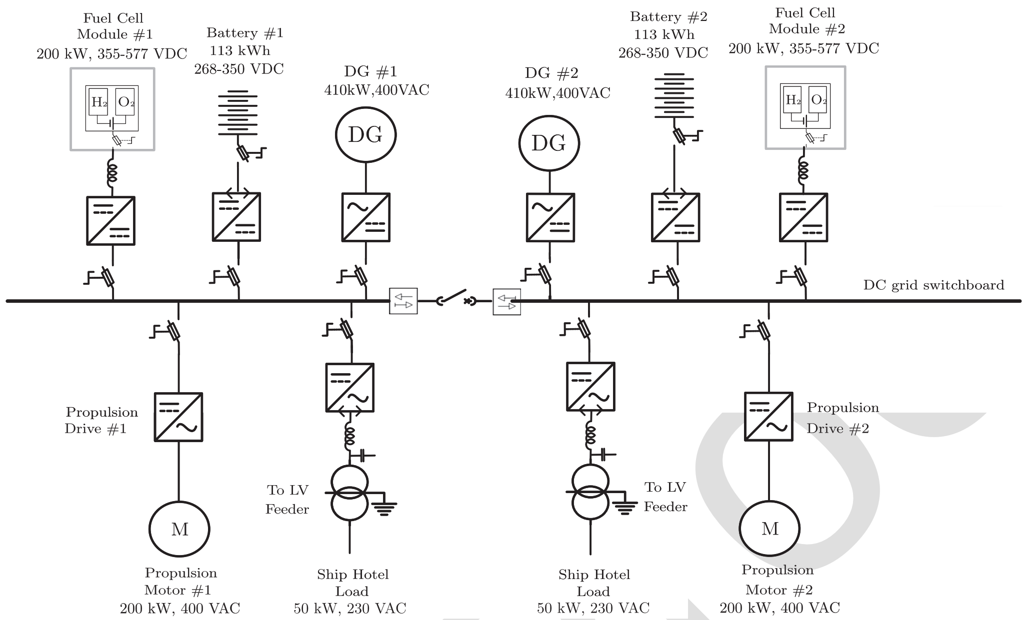

Fig. 2. Typical dc-based shipboard power system single line diagram.

the dimensions of the equipment, where the space onboard a ship is limited.

Safety is another important consideration for implementing the dc-based distribution. A dc-configured system is inherently simpler than an ac system, which means that it is easier to predict fault scenarios and devise adequate protection against them. The generators can be connected to the dc distribution system in a short time because it is not necessary for synchronization. It has considerable potential to improve the stability, efficiency, and performance of future dc-based ship power systems [18].

In addition to the benefits described above, there are numerous other benefits with dc distribution. Some of these are summarized as follows.

1) *Voltage Distortion:* Harmonic distortion is inherent in ac systems with frequency converters, while being less of a concern with dc distribution.
2) *Electrical Efficiency:* In the process of going from ac-to-dc distribution, the system efficiency is improved by 0.5–1% [19].
3) *Ease of Control:* It is not required to control the frequency and reactive power of the network. The control system is simplified and only needs to overlook the dc voltage.

Overall, the integration of a hybrid ac-distributed shipboard power is complex and costly [14]. Multiple layers of the power conversion and transmission increase the system losses and probability of equipment failure. It is more suitable for some retrofit projects, which are planned for extending a single ESS from an existing ac distribution network. Due to the advantages of dc-distribution power system, this study focuses on dc-based shipboard power plant modeling.

B. Hybrid Shipboard Power System Configuration

For a hybrid dc-distributed shipboard power system, the energy storage devices can be connected to the system. A generator set driven by a combustion diesel engine is possible to be integrated into the dc power network. Usually, synchronous generators are used and rectified (ac to dc converter) before the power is transmitted to the dc bus. Propulsion and other ship service loads are regulated by dc/ac inverters. The typical configuration of an all-electric dc hybrid ship power and propulsion system is shown in Fig. 2. In this study, two fuel cell modules are function as the main power supply to achieve zero emission operation. Two battery banks handle the ship load variations. And two diesel gen sets (DG) are the backup power in case the fuel cell devices or the hydrogen fuel are not available under emergency condition.

The main switchboards are usually split into two sections or more to obtain the redundancy requirements of the vessel according to the marine class rules and regulations. This kind of structure is not only an intrinsic advantage of dc distribution but it also has the ability to supply power to the load continuously even under certain fault conditions [16], such as short-circuit. During normal operation, the dc-grid switchboard are usually connected (close bus tie), which gives the best flexibility in the configuration of the power generation. The optimal number of the power devices can be connected to the power network according to the load transients to achieve certain control criteria.

III. Fuel Cell-Fed DC Distribution System Modeling

In this section, a system-level dc-based hybrid shipboard power plant will be modeled. The power network includes the fuel cells, batteries, and DGs as the energy sources. The essential components of the dc-grid power system are the power

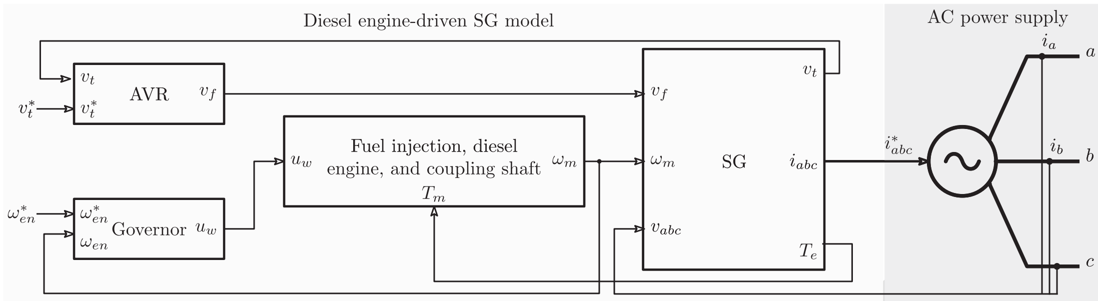

Fig. 3. General block diagram of a diesel engine-driven synchronous generator.

electronics devices. An ESS dc/dc converter and a 6-pulse ac/dc rectifier for DG integration will be modeled. The propulsion load and ship hotel loads of the vessel will be represented with controllable current sources. Power management, including load power sharing, dc voltage coordination, and power regulation will be achieved as well.

A. Energy Sources Modeling

1) *Diesel Gen-Set Model:* Fig. 3 shows the general configuration of a diesel engine-driven synchronous generator system. The system consists of four main sections: Fuel injection and diesel engine, governor, synchronous generator (SG), and automatic voltage regulator (AVR) [20]. The mathematical models of each part of diesel generator are introduced as follows.

a) *Fuel injection and diesel engine* can be presented by a time delay and the coupling shaft model, as in [21] and [22]. The simplified model is given by

$$\frac{T_m(s)}{u_\omega(s)} = \frac{K_{en} \cdot e^{-t_d \cdot s}}{t_e s + 1} \tag{1}$$

$$J_{eq} \cdot \frac{d\omega_m}{dt} = T_m - T_e - k_{f_{eq}} \cdot \omega_m \tag{2}$$

where ω_m is the mechanical speed, u_ω is the control signal from the speed governor, T_m is the mechanical torque developed by the engine, J_{eq} is the equivalent inertia of the entire system, $k_{f_{eq}}$ is the equivalent friction coefficient, K_{en} is the engine gain, t_d is a delay representing the time elapsed from the fuel injection until the torque is developed at the engine shaft, and t_e is the time constant of the fuel injection.

b) *Governor* is responsible for regulating the engine speed to maintain it within the allowable range during the different load conditions, resulting in constant output frequency or within the desired limits. This governor also has the structure of a PI controller with the droop function implemented. This model can be given by

$$u_\omega = (\omega_{en}^* - \omega_{en} - k_{dr,\text{freq}} \cdot u_\omega)\left(K_{P_\omega} + \frac{K_{I_\omega}}{s}\right) \tag{3}$$

where K_{P_ω} and K_{I_ω} are the proportional and integral gains of the governor PI controller, and ω_{en} is the engine nominal speed and $k_{dr,\text{freq}}$ is the speed droop gain that equals $(m_{dr} \cdot \omega_{en})$, and m_{dr} is the static droop slope.

c) *Synchronous generator* is considered without damper windings for the sake of simplifying the model. And its *d*-*q* rotating reference frame is given by

$$V_d = -r_s \cdot i_d + L_q \cdot \omega_e \cdot i_q + L_d \cdot \frac{di_d}{dt} + M_{sf} \cdot \frac{di_f}{dt} \tag{4}$$

$$V_q = -r_s \cdot i_q - L_d \cdot \omega_e \cdot i_d + L_q \cdot \frac{di_q}{dt} + M_{sf} \cdot \omega_e \cdot i_f \tag{5}$$

$$V_f = r_f \cdot i_f + L_f \cdot \frac{di_f}{dt} - M_{sf} \cdot \frac{di_d}{dt} \tag{6}$$

$$T_e = (L_d - L_q) \cdot i_d \cdot i_q + M_{sf} \cdot i_q \cdot i_f \tag{7}$$

where $V_d, V_q, i_d,$ and i_q are the output voltages and currents in the *d*-*q* rotating reference frame, respectively, V_f and i_f are the field excitation voltage and current, respectively, r_s and r_f are the stator winding and field winding internal resistances, respectively, L_d and L_q are the stator inductance in the *d*-axis and *q*-axis, respectively, L_f is the inductance of the field, M_{sf} is the mutual inductance between the field winding and the *d*-axis stator winding, and T_e is the electromagnetic torque. It is worth noting that, the following assumptions have been considered: The stator windings are symmetrical, a uniform sinusoidal distribution along the air gap, the permanence of the magnetic paths on the rotor is independent of the rotor positions, and the saturation and the hysteresis effects are neglected.

d) *Automatic voltage regulator* has the responsibility of controlling the terminal voltage of the synchronous generator under different load conditions. This AVR is modeled as a first-order system, representing a power converter controlled by a PI controller [20], that is given by

$$V_f = \frac{k_{\text{conv}}}{t_{\text{conv}} s + 1} \cdot (U_v - k_{dr,v} V_f) \tag{8}$$

$$U_v = \left(K_{Pv} + \frac{K_{Iv}}{s}\right) \cdot (V_t^* - V_t) \tag{9}$$

where K_{Pv} and K_{Iv} are the proportional and integral gains of the AVR PI controller, k_{conv} and t_{conv} are the

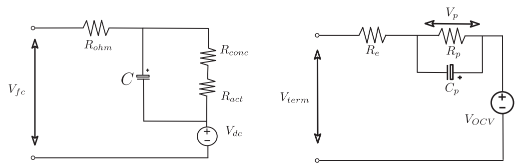

(a) (b)

Fig. 4. ESS power source modeling. (a) Proton-exchange membrane (PEM) fuel cell and its equivalent circuit. (b) Lithium-ion battery and its equivalent circuit.

converter gain and time constant, and V_t^* and V_t are the reference and measured rms output line voltage. $k_{dr,v}$ is the dc voltage droop rate for dc-distributed power system.

2) *Fuel Cell Model:* There are a few different types of fuel cell technologies. The proton-exchange membrane (PEM) fuel cell is the most mature technology over other types of fuel cell. With its relatively low cost and high energy efficiency features, PEMFC is the most widely used in marine applications [23]. Fig. 4(a) shows a single PEM fuel cell model and its equivalent circuit [24]. The fuel cell losses are mainly divided into three categories: Activation loss R_{act}, concentration loss R_{conc}, and ohmic loss R_{ohm} [25]. The voltage of a PEMFC elementary cell can be written as follows [26]:

$$V_{\text{cell}} = E_{\text{nernst}} - V_{\text{act}} - V_{\text{conc}} - V_{\text{ohm}} \tag{10}$$

$$V_{fc} = N_{fc} \times V_{\text{cell}} \tag{11}$$

where V_{cell} is the voltage of a PEMFC elementary cell, E_{nernst} is the equilibrium voltage, V_{act} is the activation overpotential, V_{conc} is the concentration overpotential, V_{ohm} is the ohmic overpotential, V_{fc} is the voltage of PEMFC stack, and N_{fc} is the number of cells in series.

In this study, the PEMFC is configured with Matlab/Simulink Simscape library.

3) *Battery Model:* To balance the cost, energy density, power density, safety performance, and life span, Li-ion battery is the most applied battery type in marine ESS applications [27]. Simple models based on the equivalent circuit of a resistor in series with a parallel *RC* circuit (polarization circuit) [28] have been used to determine the dynamic characteristics of the battery, as shown in Fig. 4(b).

Open-circuit voltage (OCV) is defined differently for discharging and charging at given state-of-charge (SoC) due to the hysteresis effect [29]. The total voltage drop from OCV is then modeled here based on the first-order equivalent circuit to account for the internal resistance and polarization (OCV relaxation).

$$V_{\text{term}} = V_{\text{OCV}} - IR_e - V_p \tag{12}$$

where V_{term} is the terminal voltage of the cell, V_{OCV} is the cell OCV, I is the current rate of the cell (positive for discharging and negative for charging), R_e is the electrical resistance (responsible for instantaneous voltage drop together with C_p, after the application of load) and V_p is the voltage drop across the polarization circuit.

At any instant, V_p across the parallel *RC* circuit is represented by the voltage drop acrossR_p or C_p. So, the equation can be arranged by

$$\frac{V_p(t)}{R_p} + C_p\frac{dV_p(t)}{dt} = I(t) \tag{13}$$

where I_{Rp} is the current across polarization resistance, and I_{Cp} is the current across polarization capacitance. The sum of I_{Rp} and I_{Cp} gives the total circuit current I.

Then perform Laplace transform by

$$V_p(s) = I(s)\frac{R_p}{1 + sR_pC_p} \tag{14}$$

so that the steady-state response of terminal voltage $V_{\text{term s}-s}$ to a given current by

$$V_{\text{terms}-s} = V_{\text{OCV}} - I(R_e + R_p) = V_{\text{OCV}} - IR_{ti} \tag{15}$$

where $R_{ti} = R_e + R_p$ is the total internal resistance of a cell.

SoC is another critical parameter for the battery system. SoC is intrinsically divided into two types: Instantaneous SoC (SoC_{inst}) and nominal SoC (SoC_{nom}), both based on Ah counting. Nominal SoC is derived from nominal capacity based on standard discharging conditions as suggested by the manufacturer, while instantaneous SoC is based on the available instantaneous discharge capacity given by

$$\text{SoC}_{\text{nom}}(t_i) = \text{SoC}_{\text{nom}}(t_{i-1}) - \frac{I_{\text{step}}(t_{i-1})t_{\text{step}}}{C_{\text{nom}}} \tag{16}$$

$$\text{SoC}_{\text{inst}}(t_i) = \frac{(1 - \text{SoC}_{\text{nom}}(t_{i-1}))C_{\text{nom}}}{C_{\text{step avail}}(t_{i-1})} - \frac{I_{\text{step}}(t_{i-1})t_{\text{step}}}{C_{\text{step avail}}(t_{i-1})} \tag{17}$$

where, I_{step} is the current at a given time step, t_{step} is the span of time under consideration (sampling time of BMS/controller), and $C_{\text{step avail}}$ is the capacity available for I_{step}. Instantaneous SoC is useful in indicating the capacity available at a given time step and operating conditions, especially higher discharge rates.

In this study, the Matlab/Simulink Simscape battery stack model is utilized.

B. Power Electronic Converter Modeling

A dc/dc converter (for fuel cell and battery control), and an ac/dc rectifier (for diesel generator control) are modeled in this section.

1) *DC/DC Converter Model:* Both of the fuel cells and the battery systems are powered by dc/dc converter. The dc/dc converter regulates the output voltage and power flow from the storage device [8]. Different from the battery bidirectional control [31], fuel cells only require a single direction power flow to provide the power to dc link. It can be represented as the following equation:

$$\frac{V_{dc}}{V_{\text{ESS}}} = \frac{1}{1 - D} \tag{18}$$

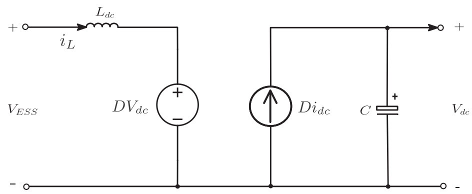

Fig. 5. DC/DC converter average model.

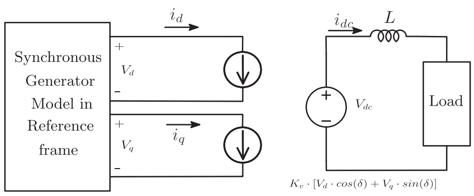

Fig. 6. Average model of 6-Pulse ac/dc rectifier, where V_d, V_q, I_d, I_q are generator's output voltage and current in $dq - axes$, δ is the angle between V_d and V_q, coefficient K_v is the ratio between the magnitude of rectifier output voltage V_{dc} and its input voltage V_d, V_q, and δ.

where D is the duty cycle of dc/dc converter.

There are two methods to model the power electronic converters, i.e., electromagnetic transient (EMT) model and average model. EMT model is straightforward and can represent the modulation process of the power electronic device. However, the simulation speed will be slow down due to the usage of high-frequency carriers during pulsewidth modulation (PWM). EMT simulation method is more suitable for system stability analysis studies, but not suitable to evaluate system performance throughout the operational profile which can last in the order minutes or even hours. For that reason, the average model is selected to configure the shipboard power plant model here. The dc/dc converter average model is shown in Fig. 5.

2) *AC/DC Rectifier Model:* The DGs are connected into dc bus via a 6-pulse diode rectifier. The average model of a diode bridge loaded synchronous generator was used here to simplify the calculation of the average values of generator *d-q* variables to the dc voltage and current at the bridge output [32], as shown in Fig. 6.

The voltage and current at the dc terminal can be defined as proportional to the amplitudes of the first harmonics of generator phase voltage and current, respectively [33]

$$V_{dc} = K_v \sqrt{V_d^2 + V_q^2} \tag{19}$$

$$i_{dc} = K_i \sqrt{i_d^2 + i_q^2} \tag{20}$$

where V_{dc} is dc voltage output from the rectifier. V_d, V_q, i_d, and i_d are the voltage and current of generator in *dq*-axes. K_v is the generator voltage constant, and K_i is the generator current constant.

C. System Control Philosophy

For existing hybrid shipboard power management is usually arranged in line with the hierarchical control framework. The basic structure is shown in Fig. 7.

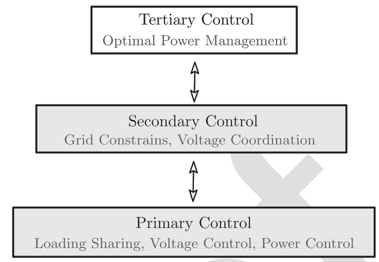

Fig. 7. Hierarchical control framework for shipboard power management, where the primary and secondary control have been applied.

In hierarchical control, the primary control level is to handle the load sharing among the hybrid power sources. The secondary control level includes the grid voltage coordination and to ensure bus signals at their operating ranges. The tertiary control level is used to achieve optimal operation with intentional objectives [34]. In this study, the primary and secondary level power management control have been achieved, while the tertiary control will be considered in future's research work.

The basic load sharing mechanism in dc-distributed power network is dc voltage droop control. Basically, with the voltage droop control, all the power sources share the load based on the dc bus voltage in the similar way as with frequency droop control in ac-distributed system. The load sharing function is realized by adjusting the voltage droop rate. In Fig. 8, it shows the load sharing results of a dc power network with three different droop rate setting. A steeper droop angle will cause one consumer to take less load than one with a more flat droop angle given the same voltage set point.

DG system is integrated into the dc network via 6-pulse diode rectifier, and the output voltage is controlled by AVR. The dc voltage set point is defined as the nominal dc voltage of the rectifier. Droop increases with increasing generator speed. Usually, the dc voltage droop rate is not larger than 5% [35].

For the energy storage power sources, such as fuel cells and batteries, the dc voltage droop control is implemented in the power electronic dc/dc converters. The block diagram of the voltage control loop is as shown in Fig. 9. It is a dual control loop, with the current control as the inner loop with the voltage control as the outer loop. $K_{dr,v}$ is the voltage droop rate for load sharing with other power sources.

The dc voltage droop control is simple and reliable. But due to the complexity of hybrid dc-grid system configuration, it is difficult to fine-tune the whole power system with one single parameter to maintain the performance of each power source, and ensure the system stability at the same time. It is also not possible to achieve strategy loading or even optimized operation. Therefore, the power control of the ESS devices is expected. The dc/dc converter power control loop with PI controllers is shown in Fig. 10. It is a single current control loop, where the current reference is given by the quotient of reference power and dc voltage.

In this study, dc voltage droop combined with power control is implemented as primary power management scheme. The system voltage coordination rules and constrains have been set in power electronic converter models as the secondary level of

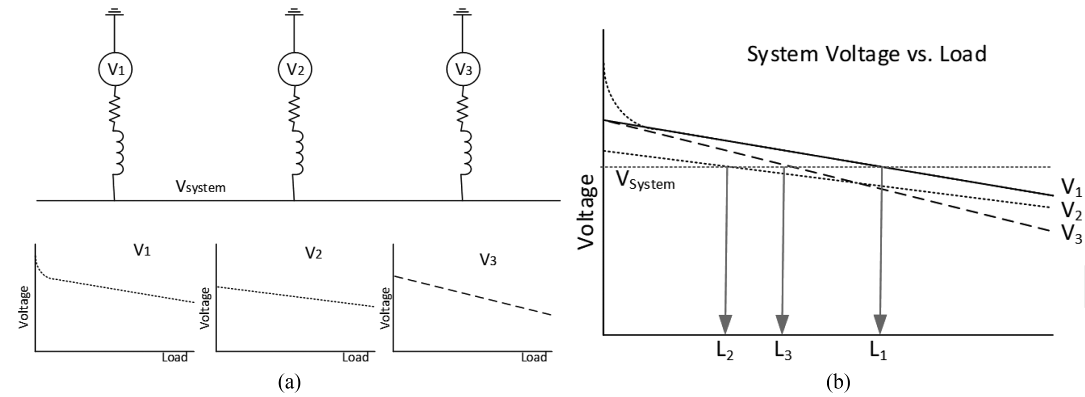

Fig. 8. Load sharing with 3 different droop curves. (a) Integrated dc-distributed system with three power sources and their droop rates. (b) System voltage and load sharing scheme.

TABLE I
PARAMETERS FOR THE DC-BASED DEMO VESSEL

Diesel-generator		**Fuel cell [30]**		**Batteries**	
Rated power (P_{gen})	410 kW	Rated power (P_{fc})	2*100 kW	Capacity (E_{batt})	113 kWh
Nominal voltage (V_{abc})	400 VAC	Min. power (P_{fc_min})	20 kW	Max. charge voltage (V_{batt_max})	350VDC
Nominal current (I_{abc})	592 A	Operating voltage (V_{fc})	355-577 VDC	Nominal voltage (V_{batt})	300 VDC
Frequency (F_n)	50 Hz	Rated current (I_{fc})	2*257 A	Min. voltage (V_{batt_min})	268 VDC
Speed (Spd)	1500 rpm	Max. Temperature (T_{max})	70°C	Max. discharge current (I_{batt_disch})	250 A
Inertia (J_{ge})	10 kgm^2	Fuel Type	Hydrogen	Max. charge current (I_{batt_ch})	200 A
Power factor (pf)	0.9	H_2 pressure	3.5-5 Barg	Operating state of charge range (SoC)	20%-80%

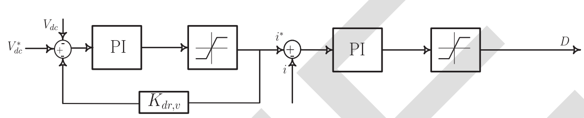

Fig. 9. DC/DC converter control scheme I - Voltage control loop.

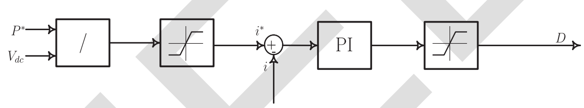

Fig. 10. DC/DC converter control scheme II - Power control loop.

power management.The ESS device output power or voltage shall be regulated according to the reference command if the corresponding control scheme is selected. Two different operation modes will be studied in this article: Zero-emission mode and DG in-parallel mode.

D. System Simulation Results

A small-scaled tugboat power plant is configured as the target vessel for simulation test. It is a typical hybrid shipboard dc-grid system design, as shown in Fig. 2. It comprises two sets of 200-kW fuel cells, two battery arrays with capacity of 113 kWh and two 410-kW DGs as the back-up power. The detailed system configuration parameters for this dc-based demo vessel are shown in Table I. The simulation tests are performed with two operating modes, respectively: Zero-emission mode and DG in-parallel mode. The test results are shown as follows.

1) *Zero-Emission Mode:* During the zero-emission mode operation, there is no DG online. The battery units are working under the voltage control scheme to regulate the system dc-grid voltage level. Two battery sets share the load via voltage droop control. Fig. 11 shows the simulation results for the dc-grid hybrid power plant performance under zero-emission operation.

a) *T = 3–15 s*: The load power increases to 300 kW. The total load demands are supplied by two fuel cell modules and two battery units. Fuel cells follow the power references from the dc/dc converter, while batteries share the remaining required power equally when the voltage droop rate is set as the same value. In this test, voltage droop rate is set as 3%.

b) *T = 15–30 s*: The propulsion load is dropped. The batteries switch to charging mode to absorb the remaining power from network for future usage.

c) *T = 30 s–end*: the load is increased to peak, around 400 kW. The batteries discharge and provide the power supply for the peak load demands.

It shows that the dynamic response of fuel cells is relatively slow and it needs the battery systems' support to fulfill the peak ship load. With voltage droop control, the system dc voltage slightly varies according to the different loading conditions. Two fuel cells are operated independently according to their own reference profiles. Usually in real practice, fuel cells can be set to provide the average load demands [36], and the batteries are to enhance the system dynamic performance and boost the power supply during peak load.

2) *DG in-Parallel Mode:* When the system is under DG in parallel mode, the DGs connect to dc network via a

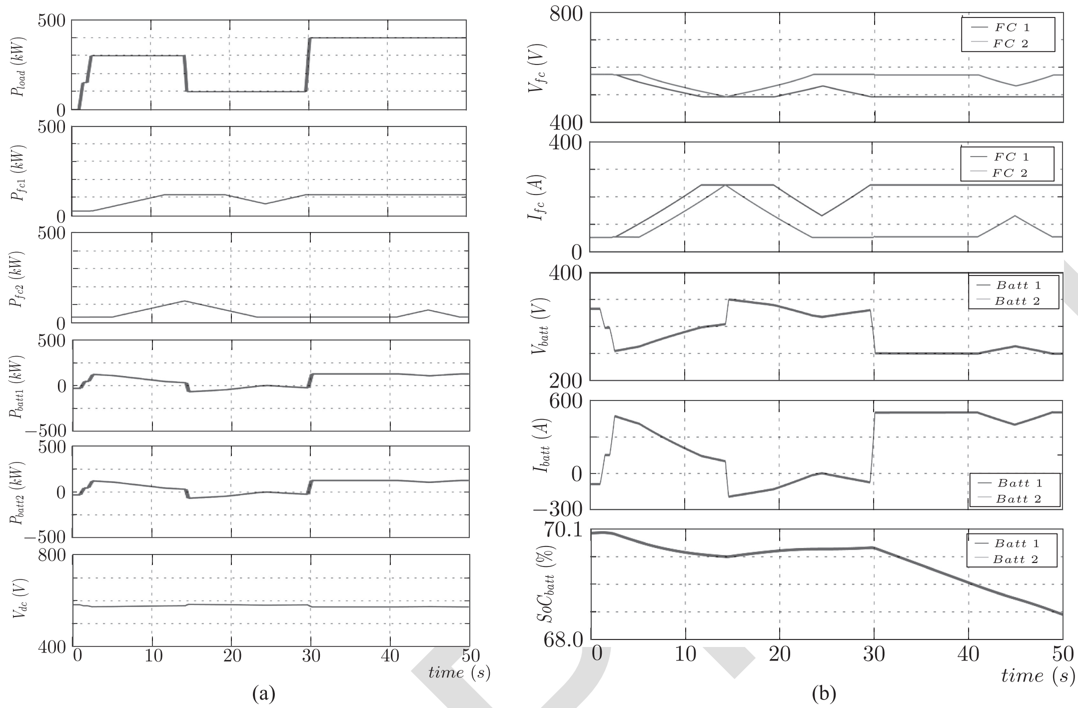

Fig. 11. Simulation results for the dc-based shipboard power grid model for demo vessel. Zero-emission mode. (a) Power split of the hybrid shipboard power plant model. (b) Dynamic behavior of fuel cell devices and batteries.

6-pulsed passive rectifier. The online diesel generators dominate the system dc voltage level naturally by its terminal ac voltage. In this case, battery systems are switched to power control scheme which is similar to the fuel cell control method to provide the output power flow as reference required to achieve an ideal loading strategy and optimization control. Fig. 12 shows the simulation results of the hybrid ship power system under DG in-parallel mode.

a) *T* = *3 - 15 s*: The load power increases to peak 400 kW. The fuel cell modules follow the power reference commands from the dc/dc converter. The propulsion load variations are absorbed and equally shared between two battery units. The voltage droop rate here is set as 2% for both the DGs so that they are able to share equal 100-kW load throughout the simulation.
b) *T* = *15 - 30 s*: The propulsion load is dropped. The batteries switch to charging mode to absorb the extra power for future usage.
c) *T* = *30 s - end*: The power of the load is shooting up to the peak again. The batteries discharge and boost the total power supply.

In this simulation test, fuel cells and battery systems provide the power supply according to the power allocation reference, and the remaining power demands from the network go to DGs online. Similar to the zero-emission mode, the batteries function as the dynamic enhancement to support the system dynamic performance. To maintain system stability, the generators shall remain stable outputs, and usually, it can be set as the average load demands.

For both zero-emission mode and DG in-parallel mode simulation test, the different power sources are integrated into the common dc-distributed power network and able to satisfy the load demands. The system power load sharing is under dc voltage droop combined with power control scheme. During both of the operation modes, the power reference profile for the two fuel cells are set differently. This system-level hybrid power plant model provides the control freedom to interface with different tertiary level power management algorithms.

IV. HIL Setup

Control algorithm testing can be time-consuming, costly, and potentially unsafe if the test is against a real hardware-based system. Therefore, software-based plant model is considered for replacing the real system and to generate the operational profile of a vessel. A HIL setup is expected to provide real-time simulation of the shipboard power system behavior and dynamics, as well as the hardwired interfaces with control signals and communication protocols. HIL test is able to ensure high quality of the control software. It is a reliable verification and validation method to prototype the controller before implementing the control algorithm into a real hardware environment [37].

In this study, the shipboard power system plant model is successfully built and run on a real-time Speedgoat target machine, which provides real-time simulation of plant model behavior and dynamics as well as the communication interface with field-bus protocols. The power and energy optimization control algorithms are developed and downloaded to a B&R brand X20CP3586 programmable logic controller (PLC)-based

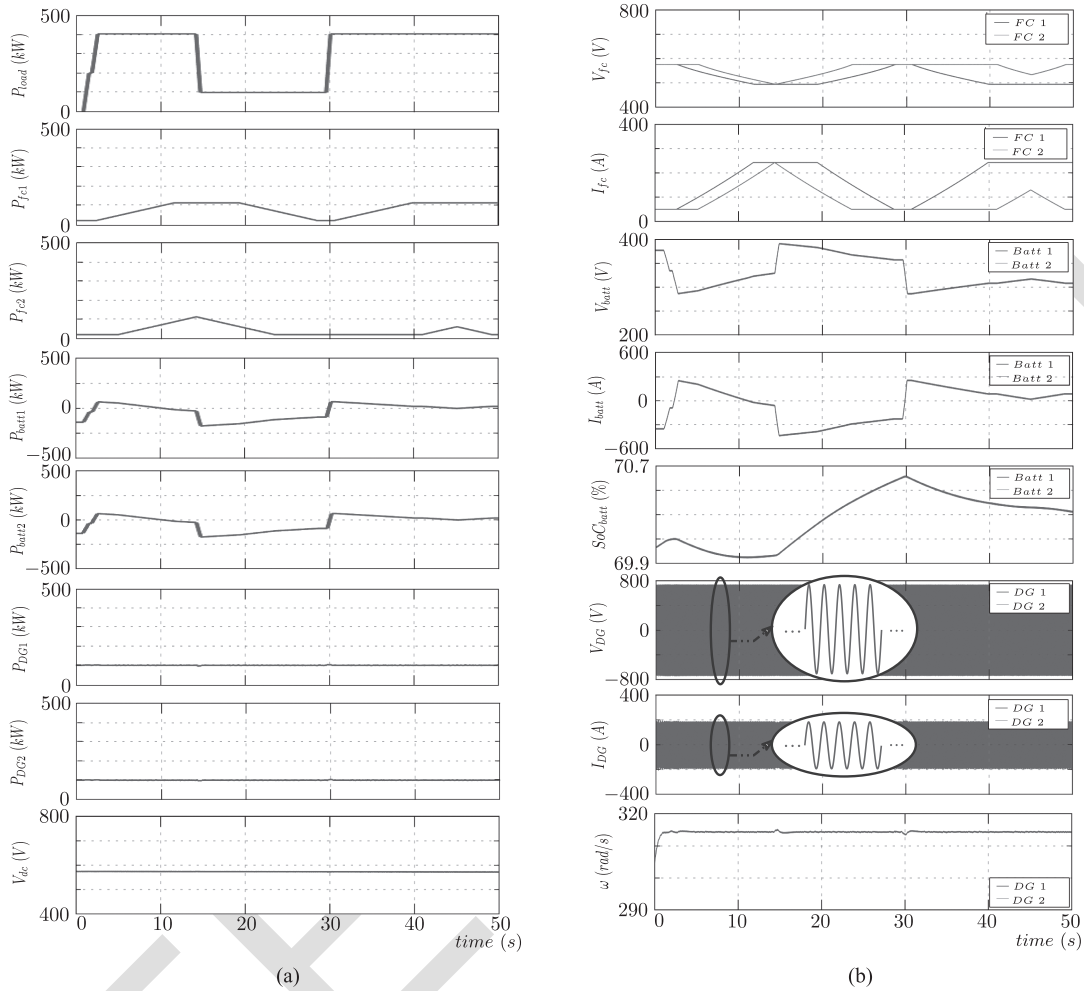

Fig. 12. Simulation results for the dc-based shipboard power grid model for demo vessel. DG in-parallel mode. Frequency of the DG is 50 Hz. (a) Power split of the hybrid shipboard power plant model. (b) Dynamic behavior of fuel cell devices, batteries and DGs.

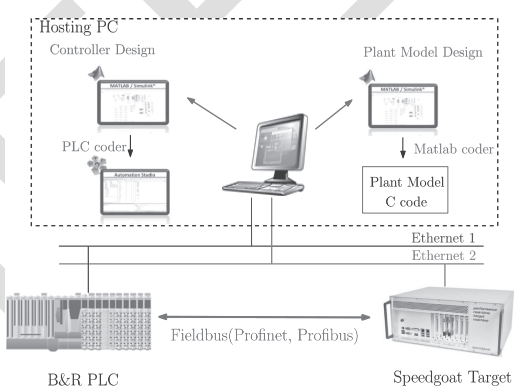

Fig. 13. HIL topology scheme.

embedded control system. The available real-time Fieldbus communication protocols between the plant model and controller are Profinet and Profibus for this setup. In this study, the topology diagram of the HIL test bed is shown in Fig. 13.

V. System Model Validation

In this study, the mathematical shipboard power system model and HIL plant are both validated against the full-scale hybrid power plant system. The actual power grid facilities are located at ABB collaborated hybrid power laboratory in MARINTEK, at Norwegian University of Science and Technology, in Trondheim, Norway. The main objective of this experimental validation test is to verify that the response of the modeled shipboard power system matches with the actual system response. The DGs and fuel cells with battery energy storage will be validated, respectively, according to the actual lab setup.

The system configuration of the MARINTEK laboratory is based on a full-scale hybrid AES with ABB onboard dc-grid system. The lab arrangement diagram is shown in Fig. 14. The lab is equipped with two 410-kW diesel engines and variable speed generator sets, two 30-kW fuel cell devices, plus one 55-kWh battery ESS. Power sources are connected to the dc-bus, and system loading conditions are simulated with two controllable electric motors. Fig. 15 shows the equipment setup in MARINTEK lab.

In the first validation test, one DG and one 55-kWh battery system are in use. The validation test results are shown in Fig. 16. The load profile is designed as four ramp-up cycles The dynamic response of a DG is limited by its mechanical characteristic, and so the battery banks are there to boost the system dynamic performance to achieve the load demands. In this test, the

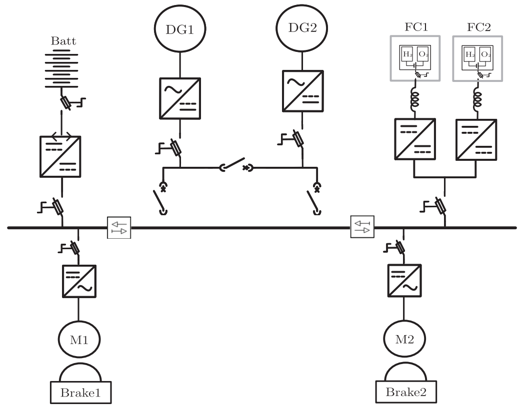

Fig. 14. ABB MARINTEK lab setup diagram, where M1 & M2 are the propulsion motors, and Brake1 & 2 present the controllable thrusters load.

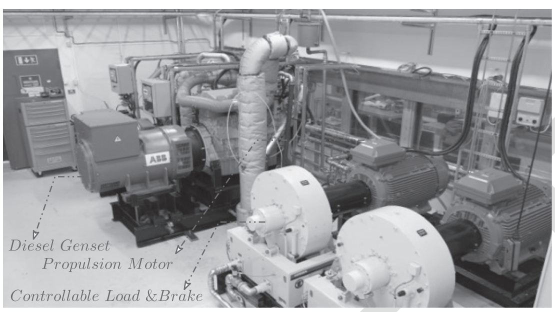

Fig. 15. ABB MARINTEK lab in Trondheim, Norway.

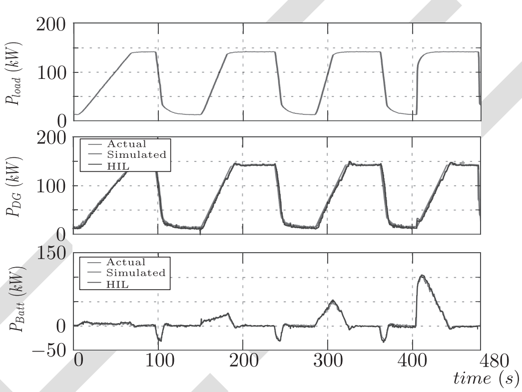

Fig. 16. Validation test I: To compare the system response between simulation model and HIL plant target in DG in-parallel mode.

simulated results from the Simulink model can match well with the actual recorded test. The overall mean average percentage error between the mathematical plant model and actual system is around 0.51%, and the average error between HIL plant and actual system is about 1.82%.

In the second validation test, two fuel cell modules and the same battery system are configured. The test results are shown in Fig. 17. During the first 100 s, the two fuel cells were powered up with 9-kW output one after another. The power drawn from the batteries was reduced with the increasing power supply from the fuel cells. From the 120 s, the load demands are reduced below the fuel cell power supply so that the batteries are charged by the fuel cells. Between 100 to 480 s, the fuel cells provide the constant power output, while the batteries absorb the load

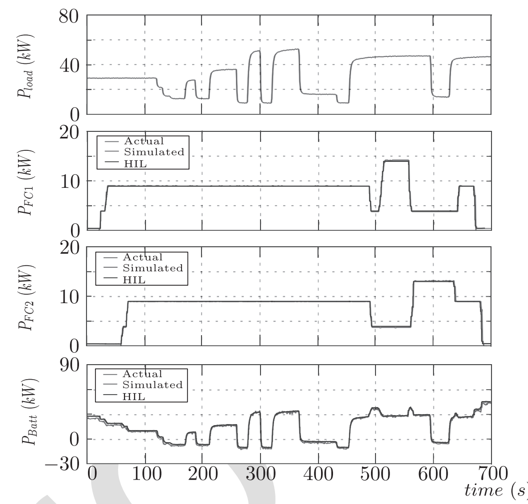

Fig. 17. Validation test II: To compare the system response between simulation model and HIL plant target in Zero-emission mode.

variations. From the 480 s onward, the power references for fuel cells are altered so that the batteries provide the remaining power to the load. The mean average percentage error is about 1.98% between the mathematical model and the actual system, while it is about 1.47% between HIL plant and the actual system.

To compare the test results, it can be seen that the system simulation and HIL results compare well with the experimental values recorded from the site. In addition, the transient rise time and steady-state power output for all DG, fuel cells, and battery power sources for both mathematical model and HIL plant can be in line with the actual system responses. Therefore, the proposed hybrid shipboard power plant model can be used to represent the physical system behavior.

VI. Conclusion

In this article, adc-distributed hybrid shipboard power system configuration has been studied. A system-level fuel cell-fed hybrid shipboard power grid system with dc distribution has been modeled. In addition, an HIL plant model platform has been set up and tested in a lab environment. Finally, both the system mathematical model and the HIL plant have been validated against a full-scale hybrid shipboard power system. This research work provides an essential platform and solid foundation to apply optimization control of power and energy management strategy in future work.

Acknowledgment

The authors would like to thank Dr. J.-F. Hansen, Dr. S. Kanerva, and their team for sharing their expertise and support to access the lab facility and data.

References

[1] *Review of Maritime Transport*, United Nations Conf. Trade Develop., Geneva, Switzerland, No. UNCTAD/RMT/2011, 2011.

[2] MARPOL, "International convention for the prevention of pollution from ships," 2019. [Online]. Available: http://www.mar.ist.utl.pt/mventura/Projecto-Navios-I/IMO-Conventions%20%28copies%29/MARPOL.pdf

[3] E. Hughes, "Initial IMO strategy on reduction of GHG emissions from ships," Int. Maritime Org., London, U.K., 2018.

[4] R. Ashdown, "The shipboard energy efficiency management plan (SEEMP)," in *Proc. IACS-EU Maritime Transp. Workshop*, 2017, pp. 2–7.

[5] C. Nuchturee and T. Li, "A review of energy efficient methods for all-electric ships," *IOP Conf. Series, Earth Environ. Sci.*, vol. 188, 2018, Art. no. 012050.

[6] P. Lin, T. Zhao, B. Wang, Y. Wang, and P. Wang, "A semi-consensus strategy toward multi-functional hybrid energy storage system in dc microgrids," *IEEE Trans. Energy Convers.*, vol. 35, no. 1, pp. 2787–2793, Mar. 2020.

[7] R. T. Amin, A. S. Bambang, C. J. Rohman, R. Dronkers Ortega, and A. Sasongko, "Energy management of fuel cell/battery/supercapacitor hybrid power sources using model predictive control," *IEEE Trans. Ind. Informat.*, vol. 10, no. 4, pp. 1992–2002, Nov. 2014.

[8] L. W. Y. Chua, "Power management for all-electric hybrid marine power systems," Ph.D. dissertation, School Mech. Aerosp. Eng. (MAE), Nanyang Technol. Uni., Singapore, 2018.

[9] J. Chen, L. Huang, C. Yan, and Z. Liu, "A dynamic scalable segmented model of PEM fuel cell systems with two-phase water flow," *Math. Comput. Simul.*, vol. 167, pp. 48–64, 2018.

[10] D. Stapersma and H. K. Woud, *Design of Propulsion and Electric Power Generation System*. London, U.K., IMarEST, 2002.

[11] R. E. Hebner *et al.*, "Technical cross-fertilization between terrestrial microgrids and ship power systems," *J. Modern Power Syst. Clean Energy*, vol. 4, no. 2, pp. 161–179, Apr. 2016.

[12] S. Fang, Y. Wang, B. Gou, and Y. Xu, "Toward future green maritime transportation: An overview of seaport microgrids and all-electric ships," *IEEE Trans. Veh. Technol.*, vol. 69, no. 1, pp. 207–219, Jan. 2020.

[13] W. Chen *et al.*, "On the modelling of fuel cell-fed power system in electrified vessels," in *Proc. IEEE 21st Workshop Control Model. Power Electron.*, 2020, pp. 1–8.

[14] M. Al-falahi, T. Tarasiuk, S. Jayasinghe, Z. Jin, H. Enshaei, and J. Guerrero, "Microgrids: Control and power management optimization," *Energies*, vol. 11, 2018, Art. no. 1458.

[15] Z. Jin, L. Meng, J. M. Guerrero, and R. Han, "Hierarchical control design for a shipboard power system with dc distribution and energy storage aboard future more-electric ships," *IEEE Trans. Ind. Informat.*, vol. 14, no. 2, pp. 703–714, Feb. 2018.

[16] P. W. Tomislav Dragicevic and F. Blaabjerg, *DC Distribution Systems and Microgrids*. London, U.K.: Inst. Eng. Technol., 2018.

[17] A. Haxhiu, A. Abdelhakim, S. Kanerva, and J. Bogen, "Electric power integration schemes of the hybrid fuel cells and batteries-fed marine vessels—An overview," *IEEE Trans. Transport. Electrific.*, to be published, doi: 10.1109/TTE.2021.3126100.

[18] J. P. Trovão, F. Machado, and P. G. Pereirinha, "Hybrid electric excursion ships power supply system based on a multiple energy storage system," *IET Elect. Syst. Transp.*, vol. 6, no. 3, pp. 190–201, 2016.

[19] "Onboard DC grid: The step forward in power generation and propulsion," ABB AS, Billingstad, Norway, 2013.

[20] *IEEE Recommended Practice for Excitation System Models for Power System Stability Studies*, IEEE Standard 421.5–2016 (Revision of IEEE Std 421.5-2005), 2016.

[21] S. Roy, O. P. Malik, and G. S. Hope, "A low order computer model for adaptive speed control of diesel driven power-plants," in *Proc. Conf. Rec. IEEE Ind. Appl. Soc. Annu. Meeting*, 1991, pp. 1636–1642.

[22] M. A. Rahman, A. M. Osheiba, T. S. Radwan, and E. S. Abdin, "Modelling and controller design of an isolated diesel engine permanent magnet synchronous generator," *IEEE Trans. Energy Convers.*, vol. 11, no. 2, pp. 324–330, Jun. 1996.

[23] T. Tronstad, H. H. Åstrand, G. P. Haugom, and L. Langfeldt, "DNV-GL EMSA study on the use of fuel cells in shipping," EMSA European Maritime Safety Agency, 2017. [Online]. Available: https://www.studocu.com/en-gb/document/brunel-university-london/energy-conversion-technologies/emsa-study-on-the-use-of-fuel-cells-in-shipping/5956606

[24] L. Kong, J. Yu, and G. Cai, "Modeling, control and simulation of a photovoltaic/hydrogen/supercapacitor hybrid power generation system for grid-connected application," *Int. J. Hydrogen Energy*, vol. 44, no. 46, pp. 25129–25144, 2019.

[25] M. İnci, M. Büyük, M. M. Savrun, and M. H. Demir, "Design and analysis of fuel cell vehicle-to-grid (FCV2G) system with high voltage conversion interface for sustainable energy production," *Sustain. Cities Soc.*, vol. 67, 2021, Art. no. 102753.

[26] M. M. Savrun and M. İnci, "Adaptive neuro-fuzzy inference system combined with genetic algorithm to improve power extraction capability in fuel cell applications," *J. Cleaner Prod.*, vol. 299, 2021, Art. no. 126944.

[27] B. Perry, "High capacity battery packs," ABB Generation, white paper, 2019. [Online]. Available: https://library.e.abb.com/public/82b8e284d5fdc935c1257a8a003c26a4/ABB%20Generations_22%20High%20capacity%20battery%20packs.pdf

[28] J. Gao, S.-Q. Shi, and H. Li, "Brief overview of electrochemical potential in lithium ion batteries," *Chin. Phys. B*, vol. 25, no. 1, Jan. 2016, Art. no. 018210.

[29] M. Farag, "Lithium-ion batteries: Modelling and state of charge estimation," Ph.D. dissertation, Dept. Mech. Eng., McMaster Univ., Hamilton, ON, Canada, 2013.

[30] "PEM fuel cell module for heavy duty motive applications–Product data sheet," Ballard, Burnaby, BC, Canada, 2018. [Online]. Available: https://hfcnexus.com/wp-content/uploads/2016/07/Ballard-FCmove-data-sheet.pdf

[31] W. Chen, A. K. Ådnanses, J. F. Hansen, J. O. Lindtjørn, and T. Tang, "Super-capacitors based hybrid converter in marine electric propulsion system," in *Proc. 19th Int. Conf. Elect. Mach.*, 2010, pp. 1–6.

[32] H. Zhu, "New multi-pulse diode rectifier average models for AC and DC power systems studies," Ph.D. dissertation, Bradley Elect. Comput. Eng. Dept., Virginia Polytech. Inst. State Univ., Blacksburg, VA, USA, 2005.

[33] I. Jadric, D. Borojevic, and M. Jadric, "A simplified model of a variable speed synchronous generator loaded with diode rectifier," in *Proc. Rec. 28th Annu. IEEE Power Electron. Specialists Conf., Formerly Power Conditioning Specialists Conf. Power Process. Electron. Specialists Conf.*, 1997, vol. 1, pp. 497–502.

[34] J. M. Guerrero, J. C. Vasquez, J. Matas, L. G. de Vicuna, and M. Castilla, "Hierarchical control of droop-controlled AC and DC microgrids-A general approach toward standardization," *IEEE Trans. Ind. Electron.*, vol. 58, no. 1, pp. 158–172, Jan. 2011.

[35] F. Thams, S. Chatzivasileiadis, and R. Eriksson, "DC voltage droop control structures and its impact on the interaction modes in interconnected AC-HVDC systems," in *Proc. IEEE Innov. Smart Grid Technol. - Asia Proc. IEEE Innov. Smart Grid Technol.- Asia*, 2017, pp. 1–6.

[36] A. Rabbani, "Dynamic performance of a PEM fuel cell system," Ph.D. dissertation, Tech. Univ. Denmark, Kongens Lyngby, Denmark, 2019.

[37] D. J. Murray-Smith, "Real-time simulation, virtual prototyping and partial-system testing," in *Modelling and Simulation of Integrated Systems in Engineering*. Sawston, U.K.: Woodhead, 2012.

Wenjie Chen (Student Member, IEEE) received the B.Sc. degree in automation from Shanghai Maritime University, Shanghai, China, in 2007, the M.Sc. degrees in electrical engineering from Ecole Polytechnique de l'Université de Nantes, France, in 2009. She is currently working toward the Ph.D. degree in optimization control for power system under the supervision of Prof. K. Tai with Nanyang Technological University, Singapore, and Prof. T. Tjahjowidodo with Katholieke Universiteit Leuven, Leuven, Belgium, since January 2019.

She firstly joined ABB China (Shanghai) in 2010, and then transferred to ABB Singapore in 2011. Currently, she is based in Singapore as a Research Specialist.

Kang Tai received the B.Eng. degree in mechanical engineering from the National University of Singapore, Singapore, and the Ph.D. degree from Imperial College, London, U.K.

He is currently an Associate Professor with the School of Mechanical and Aerospace Engineering, Nanyang Technological University, Singapore. His research interests include optimization, evolutionary computation, mathematical/empirical modeling of industrial processes, and analysis of interdependencies, risks and vulnerabilities in critical infrastructure networks.

Michael Lau received the Ph.D. degree in mechanical engineering from Aston University, Aston, U.K. and the C.Eng. degree from Institution of Mechanical Engineers, London, U.K.

He was a Control and Instrument Engineer with Ministry of Defence, Singapore, and later with an oil and gas industry for about four years, before spending the next 35 years as an academician, first with Nanyang Technological University, Singapore, until 2010, and then with Newcastle University in Singapore (NUiS), Singapore till current. He is currently an Associate Professor with NUiS. His research interests include control, mechatronics system designs and energy systems.

Ahmed Abdelhakim (Senior Member, IEEE) was born in Egypt on April 1, 1990. He received the B.Sc. and the M.Sc. degrees (with hons.) in electrical engineering from Alexandria University, Alexandria, Egypt, in 2011 and 2013 respectively, and the Ph.D. degree from the University of Padova, Vicenza, Italy, in 2019.

He is currently with ABB Research Sweden as a Principal Scientist Scientist and R&D Project Manager. His research interests include power electronics converters and their applications for fuel cells and energy storage systems, investigation of new power converter topologies, and application of wide-bandgap semiconductor devices (GaN/SiC) for high frequency and high-power density power converters.

Dr. Abdelhakim was the recipient of the classified excellent Ph.D. dissertation award from Societá Italiana di Electronica (SIE'19) among Italian Universities, in 2019. He serves as an Associate Editor for the IEEE TRANSACTION ON INDUSTRIAL ELECTRONICS and IEEE TRANSACTION ON TRANSPORTATION ELECTRIFICATION.

Ricky R. Chan received the Ph.D. degree in electrical engineering from Purdue University, West Lafayette, IN, USA, in 2009.

He is currently a Research and Development Manager with ABB Marine & Ports in Helsinki, Finland, where he leads a team of specialists in the development of advanced electric solutions for marine applications.

Alf Kåre Ådnanes received the M.Sc. and Ph.D. degrees in electrical engineering from the Norwegian University of Science and Technology, Trondheim, Norway.

He heads the regional division in AMEA of ABB Marine & Ports. He joined ABB in 1991, and among previous positions with ABB, he has worked within corporate research, and various positions within Marine, including delivery projects, engineering, and in product management and development, and technology management for the global marine business unit for Marine & Ports.

Tegoeh Tjahjowidodo received the Ph.D. degree in mechanical engineering and automation from KU Leuven, Belgium in 2006.

He is currently an Associate Professor with the Department of Mechanical Engineering, KU Leuven. From 2009 until 2019, he has been with the School of Mechanical & Aerospace Engineering, Nanyang Technological University, Singapore, as an Associate Professor. His research interests include nonlinear dynamics, modeling, identification and control, with more focus in monitoring for manufacturing.